



NLR TP 97153

**Review of aeronautical fatigue investigations in
the Netherlands during the period
March 1995-March 1997**

J.B. de Jonge

DOCUMENT CONTROL SHEET

	ORIGINATOR'S REF. NLR TP 97153 U		SECURITY CLASS. Unclassified										
ORIGINATOR National Aerospace Laboratory NLR, Amsterdam, The Netherlands													
TITLE Review of aeronautical fatigue investigations in the Netherlands during the period March 1995-March 1997													
PRESENTED AT the 25th ICAF Conference, Edinburgh, United Kingdom, 16-17 June 1997													
AUTHORS J.B. de Jonge		DATE 970312	<table style="width: 100%; border: none;"> <tr> <td style="text-align: center;">pp</td> <td style="text-align: center;">ref</td> </tr> <tr> <td style="text-align: center;">37</td> <td style="text-align: center;">42</td> </tr> </table>	pp	ref	37	42						
pp	ref												
37	42												
DESCRIPTORS <table style="width: 100%; border: none;"> <tr> <td style="width: 50%;">Airframe materials</td> <td style="width: 50%;">In-flight monitoring</td> </tr> <tr> <td>Crack propagation</td> <td>Laminates</td> </tr> <tr> <td>Damage assessment</td> <td>Netherlands</td> </tr> <tr> <td>Fatigue life</td> <td>Research projects</td> </tr> <tr> <td>Gust loads</td> <td>Summaries</td> </tr> </table>				Airframe materials	In-flight monitoring	Crack propagation	Laminates	Damage assessment	Netherlands	Fatigue life	Research projects	Gust loads	Summaries
Airframe materials	In-flight monitoring												
Crack propagation	Laminates												
Damage assessment	Netherlands												
Fatigue life	Research projects												
Gust loads	Summaries												
ABSTRACT A brief review is given of work performed in the Netherlands in the field of aeronautical fatigue. Where possible, applicable references have been presented.													



Summary

A brief review is given of work performed in the Netherlands in the field of aeronautical fatigue. Where possible, applicable references have been presented.

Contents

1.1	INTRODUCTION	5
1.2	LOADS	5
1.2.1	Reanalysis of Fokker F27 and F28 operational acceleration data	5
1.2.2	Fokker 100 operational tailloads	5
1.2.3	Fatigue loads/usage monitoring of military aircraft	6
1.2.4	Engine usage monitoring	7
1.3	CRACK GROWTH AND DAMAGE TOLERANCE STUDIES	7
1.3.1	A new crack growth equation for prediction of frequency and threshold effects in corrosion fatigue	7
1.3.2	Assessment of stress intensity factors in threaded rods and bolt/nut assemblies	7
1.3.3	Part through cracks and oblique through cracks in riveted lap joints	7
1.3.4	NASGRO/ESACRACK model improvement, implementation and verification	7
1.3.5	Fatigue crack growth in Inconel 718	8
1.4	FATIGUE STUDIES	8
1.4.1	Cumulative fatigue damage aspects	8
1.4.2	Applicability of the crack severity index (CSI) for fatigue crack initiation	8
1.4.3	Fatigue and fracture of Aluminium Alloys	8
1.4.4	Fatigue and Fracture in an Aircraft Engine Pylon	9
1.4.5	Effect of countersink edge corrosion on fatigue crack initiation	9
1.4.6	Cadmium substitution in aircraft	9
1.4.7	Three dimensional finite element analysis of three rivet row lap splice joint	10
1.4.8	Fatigue of riveted 2024-T3 and GLARE lap joints	10
1.5	FULL SCALE FATIGUE TESTS	10
1.5.1	Fokker 100 horizontal stabilizer-fin tear down inspection	10
1.5.2	Fokker 100 wing/fuselage damage tolerance test	11
1.5.3	Fokker 60 fatigue and damage tolerance component tests	11
1.5.4	Gulfstream V horizontal stabilizer fatigue and damage tolerance test	12
1.5.5	Full scale fuselage panel tests	13
1.5.6	Testing the centre section of a composite stabilizer	13
1.5.7	Definition of gust test load conditions for fatigue tests	14
1.6	AGEING AIRCRAFT	15
1.6.1	Structural Maintenance of Ageing Aircraft (SMAAC)	15
1.6.2	Corrosion Fatigue	15
1.6.3	Residual strength tests on stiffened panels with multiple cracks	16
1.6.4	Prediction of residual strength in panels with multiple collinear cracks	16
1.7	FIBER METAL LAMINATES	16
1.7.1	The damage tolerance behaviour of riveted GLARE3-3/2-0.2 lap joints	16
1.7.2	Repair with bonded fibre metal laminate patches	17
1.7.3	Stable static crack growth in GLARE, R-curves	17
1.7.4	Spliced Fibre Metal Laminates	17
1.7.5	Fatigue tests on small fiber-metal laminates specimens	17
1.7.6	Fatigue investigation of Structural Laminates Company, SLC	18
1.8	REFERENCES	19

2 Tables
22 Figures

(37 pages in total)

1.1 INTRODUCTION

The present review gives a brief summary of the work performed in the Netherlands in the field of Aeronautical fatigue during the period from March 1995 until March 1997. The various contributions to this review come from the following sources:

- The National Aerospace Laboratory (NLR).
- The Faculty of Aerospace Engineering, Delft University (TU Delft).
- Fokker Services.
- Fokker Aerostructures.
- Structural Laminates Company (SLC).

The names of the principal investigators and their affiliation are presented between brackets at the end of each topic title.

1.2 LOADS

1.2.1 Reanalysis of Fokker F27 and F28 operational acceleration data (J.B. de Jonge, NLR)

In order to check the validity of the assumed design spectra for the Fokker F27 and F28 aircraft, the Netherlands Civil Airworthiness Authorities RLD required counting accelerometers to be installed in operational aircraft. Between 1961 and 1976 at least on aircraft in the fleet of each operator was equipped with an accelerometer of the "Fatiguemeter" type.

These meters were read out on a monthly or weekly basis and the recorded data sent to Fokker's for further processing and analysis. When these measurements were stopped, a very large data base had been accumulated, covering for the F27 about 320000 flights, from 63 aircraft operated by 29 operators, and for the F28 150000 flights, 38 aircraft and 25 operators.

Within the framework of the cooperation between the FAA and the Netherlands Airworthiness Authorities RLD, this very large data base has been reanalyzed to study the scatter in load experience between aircraft of the same type, but used by different operators serving different networks.

Figure 1 illustrates the amount of variation in load factor experience per flight. To quantify the variation in load factor experience in terms of fatigue damage, a "Damage Index" DI was defined, based on a simple Miner Type damage calculation for the wing root lower wing skin area.

Figure 2 illustrates the amount of variation found in average DI between different aircraft. The coefficient of variation in the average damage per flight between different operators is about .35. The results of the present analysis give a quantified illustration of the reduction in inspection effort that could be obtained for transport aircraft if the inspection schemes could be adapted on the basis of individual aircraft load monitoring (Ref. 1).

1.2.2 Fokker 100 operational tailloads (P.A. van Gelder, NLR)

In order to obtain statistical information about actual tail loads in service and to check the validity of current procedures for defining design tail load spectra, NLR has carried out tail load measurements on a Fokker 100 aircraft during operational flights.

Tail loads in terms of bending moments at the stabilizer root have been measured by means of strain gauges, lateral acceleration at the rear part of the fuselage is measured by an accelerometer. The measured signals are searched for peaks and valleys that are stored with a time-mark on a solid state memory of a small micro processor based data recorder (SPECTRAPOT 4C).

The data is combined and synchronized with a selection of aircraft and flight parameters that are obtained from the Aircraft Condition Monitoring System (ACMS). In this way a unique load recording procedure is realized that is easy to install and does not interfere with other aircraft systems or handling procedures. A description of the creation and contents of the database is given in [2]. Halfway 1995 a database with 2063 flights had been established.

In 1995 and 1996 the analysis of the data was carried out with special attention to the comparison between measured fatigue load spectra and the load spectra that have been applied in the full-scale fatigue test. Also the assumptions used to derive the fatigue load spectra have been checked for validity, and the conservatism applied to these

assumptions has been confirmed, bearing in mind that the results apply to only one operator and one particular type of operation [3, 4].

In another part of this analysis a derivation has been performed of the lateral and vertical gust statistics, both for discrete and continuous gust [5].

In figures 3 and 4 some results have been presented for two low-altitude bands, where most gusts have been encountered and for a frequently used cruising altitude.

From the results it is concluded that lateral and vertical gusts are very much alike when continuous gust is considered (Fig. 4). The derived discrete gust statistics showed large discrepancies between lateral and vertical gusts (Fig. 3).

1.2.3 Fatigue loads/usage monitoring of military aircraft

a. Structural fatigue load monitoring of RNLAf F-16 aircraft (D.J. Spiekhout, NLR)

The Fatigue Load Monitoring programme of F-16 aircraft of the Royal Netherlands Air Force (RNLAf) has been continued. In the current programme, three aircraft within each squadron are equipped with a four-channel digital solid state recorder measuring wing root bending moment and three additional load quantities.

From these measurements, average spectra per mission type and per squadron are calculated.

The RNLAf has recently procured the new "Fatigue analysing and Air Combat Evaluation system (FACE)" developed by RADA Electronics Industries Ltd. in Israel to be installed in all F-16 aircraft. This system will allow a more extensive load monitoring on individual aircraft basis. Quantities measured to monitor structural fatigue loading include strains in five different structural locations ("monitoring points") and a number of flight parameters. The implementation of this new system in the fleet has started and the system will become fully operational in 1997.

b. Derivation of multiple linear regression equations between wing root loads and flight parameters for the TuAF F-16C (J. Laméris, NLR)

As part of a collaborative Developing Defense Industries (DDI) project between the Turkish Air Force (TuAF) and the National Aerospace Laboratory (NLR) the wing root area of one TuAF F-16C aircraft has been instrumented with six strain gauge bridges. Additionally ten flight parameters, like altitude, speed and vertical acceleration, have been measured. This study describes the development of the load equations to predict the shear, bending moment and pitching moment in the root of the wing based on the output of these flight parameters and their derivatives. These load equations have been generated for two different store configurations. These load equations were derived with multiple linear regression analysis and are based on flight tests conducted between October 1994 and February 1996.

It is intended to use the test data for a comparison of the multiple regression analysis with an analysis based on artificial neural networks, to be performed in 1997-1998 [6, 7].

c. Operational load measurements in Orion aircraft (A.A. ten Have, NLR)

As part of a collaborative DDI project between the Portuguese Air Force and the NLR, one Orion aircraft of the Portuguese Air Force and one of the Royal Netherlands Navy have been instrumented with a 8-channel flight load data recorder. The parameters recorded include basic flight parameters (V,G,h, cabin pressure etc.) and bending strains in three wing sections.

The recorded data will be used to evaluate the basic load-experience assumptions underlying current fatigue life monitoring on the basis of usage parameters and to study specific aspects of the operational usage in both countries.

d. POAF A-7P Load Monitoring (A.A. ten Have, J.A.J.A. Dominicus, NLR)

As part of another collaborative DDI project between the Portuguese Air Force and NLR, operational flight load measurements in a Portuguese A-7P aircraft were carried out, using an eight-channel data recorder. Recorded quantities included strain histories in two wing locations.

The measurements were used to develop two load/time histories representing Portuguese usage. Crack growth calculations for the mentioned wing locations under these load histories were made, using different crack growth prediction techniques. The results were compared with crack growth test results, obtained from tests on simply notched specimens [8, 9].

1.2.4 Engine usage monitoring (A.A. ten Have and J.H. Heida, NLR)

Since 1990, NLR performs operational engine usage monitoring of Pratt & Whitney F100 engines installed in the F-16. For this purpose, a number of multi-channel data-acquisition systems have been installed in the RNLAf F-16 fleet registering parameters such as pressure altitude, airspeed, engine rotational speed and power lever angle (PLA). Engine damage accumulation is then calculated from the recorded engine cycles using specific algorithms. Furthermore, flight time and hot time envelopes (time spent in certain Mach number versus altitude regions) are determined. To date, more than 9000 RNLAf F-16 sorties have been collected. On a routine basis, this operational RNLAf engine data is transferred to the engine manufacturer for evaluation purposes and to serve as a basis for tailored engine maintenance procedures, e.g. affecting inspection intervals or retirement lives.

In 1997, further work is planned to introduce the Fatigue Analysing and Air Combat Evaluation system (FACE) developed by RADA Electronic Industries Ltd. in Israel. This system enables the recording of approximately 100 engine parameters of which a representative selection will be made.

1.3 CRACK GROWTH AND DAMAGE TOLERANCE STUDIES

1.3.1 A new crack growth equation for prediction of frequency and threshold effects in corrosion fatigue (A.U. de Koning, NLR)

The assumption is made that accelerated fatigue crack growth due to environmental effects may occur when the strain rate at the crack front exceeds a critical value. Using an incremental crack growth law that relates an increment of crack size to the increments of stress intensity factor and time, the crack growth rate per load cycle is calculated by integration in the load and time domains. The equations were used to reproduce some experimental results found in the open literature.

A similar formulation for sustained load crack growth (including stress corrosion cracking) is under development.

1.3.2 Assessment of stress intensity factors in threaded rods and bolt/nut assemblies (A.U. de Koning, NLR)

A series of 3D FEM analyses were executed to calculate stress intensity factor distributions for different crack shapes and sizes. All cracks were assumed to be in the neck of the severely loaded bolt thread near the thread runout of the nut. Loading of the FEM model is in tension and in bending. Using an analytical bar model, attached to the FEM model, the effect of shank length was included. The results were implemented in the NASGRO and ESACRACK software for damage tolerance analyses [10, 11].

1.3.3 Part through cracks and oblique through cracks in riveted lap joints (S. Fawaz, TU Delft)

FE calculations were made to obtain stress intensity factors for hole edge cracks under different loading conditions: unidirectional and biaxial tension, bending and pin loading. Small quarter elliptical part through cracks and oblique through cracks with an elliptical crack front were considered. A large amount of results is now evaluated for prediction purposes. The FE technique is discussed in [12]. The cooperation with NASA (Dr. Newman) should be acknowledged.

In parallel, the development of cracks in riveted lap joints is now studied by fractographic observations in the electron microscope. Marker loads are used for this purpose.

1.3.4 NASGRO/ESACRACK model improvement, implementation and verification (A.U. de Koning, NLR)

The strip-yield model was further improved by assuming constrained effects that may vary with the position in the plastic zone.

Further, the loads definition was improved. In the previous versions of the software loads were defined in the form of

a series of spectra. A definition in the form of a sequence of load reversal points was added as well as modules for "rain flow" counting and -synthesis. This allows to make conversions from the sequence to the spectra definition and vice versa. The data base management software (CGDBMAN) was further improved and extended. This system allows to execute many verifications (thousands) and repeat such calculations. Results obtained using different models can be compared and plotted together with available experimental results (da/dn-a and a-N).

In the loads generation module the following options are available now: ESALOAD, F27, F100, F16 Hot- and Cold Turbistan, User defined sequences and spectra [13, 14].

1.3.5 Fatigue crack growth in Inconel 718 (R.J.H. Wanhill, J.A.M. Boogers and H.J. Kolkman, NLR)

As part of a collaborative project an investigation was made of fatigue life and fatigue crack growth in the nickel-based superalloy Inconel 718 at 600 °C [15]. The stress waveforms applied included sinusoidal waveforms, trapezoidal waveforms with and without dwells and with or without peak loads at the onset or the end of the dwell and the "Hot and Cold Turbistan" standardized fatigue test loading sequence for tactical aircraft cold section engine discs. The test types were strain controlled LCF tests on smooth specimens and fatigue crack growth tests on compact tension, rim and corner crack specimens. An optical crack measurement system was developed to study growth of short cracks. The fracture surfaces were studied by means of Scanning Electron Microscopy. Conclusions were:

- * Large superficial blocky NbC particles played an important role in fatigue crack initiation, except for the rim specimens which contained very small starter notches.
- * LCF crack growth exhibited a "short crack effect" for cyclic plastic zone sizes smaller than the mean grain size. The crack growth rate varied with a period equal to the mean grain size.
- * Intergranular dwell cracking (grain boundary oxidation followed by the cracking of the embrittled grain boundaries) was the dominant crack growth mechanism for high R values, high temperatures or long dwell times. Slower transgranular fatigue crack growth was promoted by the reverse conditions. Creep crack growth did not play a role.
- * For dwell cycling with peak loads at 600 °C and with $R = 0.1$ the crack growth was determined by ΔK deduced from the stress during the dwells rather than ΔK deduced from the peak stress.
- * For dwell cycling at 600 °C the parameter controlling the fatigue crack growth rate for $R = 0.5$ and $R = 0.7$ was K_{max} instead of ΔK .

1.4 FATIGUE STUDIES

1.4.1 Cumulative fatigue damage aspects (J. Schijve, TU Delft)

A chapter was prepared for volume 19 of the Materials handbook of the American Society for Metals [16]. The topic is "mechanisms and theory of fatigue crack growth under variable-amplitude loading". Another paper was prepared for the Fatigue'96 conference in Berlin [17].

As part of a flight-simulation program a selective Rain-Flow filter has been proposed and will be evaluated in a test program. It is based on a ΔS_{eff} criterion.

1.4.2 Applicability of the crack severity index (CSI) for fatigue crack initiation (J. Laméris and L. Schra, NLR)

An experimental test programme has been conducted to investigate whether the crack initiation life of different fighter-type load spectra can be ranked with the (Spectrum) Crack Severity Index, (S)CSI. Based on results with dogbone specimens with a central hole and four different F16 load sequences it is concluded that the CSI concept is better suited for ranking crack growth lives than for crack initiation lives, see figure 5. Excluding the effect of retardation by setting the minimum opening stress to zero improved the correlation of CSI calculations for crack initiation and thus fatigue life with about 7 percent compared to the original CSI calculations. The CSI concept with assumed minimum opening stress level was found to be comparable with Palmgren-Miner damage calculations in terms of ranking the fatigue lives of the four F16 spectra studied [18].

1.4.3 Fatigue and fracture of Aluminium Alloys (R.J.H. Wanhill, NLR)

NLR Technical Publication TP 94177, "Damage Tolerance Engineering Property Evaluations of Aerospace

Aluminium Alloys with Emphasis on Fatigue Crack Growth", was submitted as a Doctor's Thesis to Delft University of Technology. The report describes and evaluates, in more than 850 pages, the results of more than 20 years' work at the NLR on high strength aluminium alloys. Copies of the report have been sent to member countries of ICAF and to a number of international companies and institutes [19].

1.4.4 Fatigue and Fracture in an Aircraft Engine Pylon (R.J.H. Wanhill, A. Oldersma, NLR)

In 1992 separation of an engine from an El Al 747-200 cargo aircraft resulted in a catastrophic accident near Amsterdam. The engine separated, together with its pylon, owing to fatigue and fracture of components connecting the pylon to the wing. In NLR Technical Publication TP 96719 the NLR's investigation of the pylon components is reviewed, and contributions from other investigations are included in order to describe the most probable cause and sequence of damage leading to separation of the engine and pylon. Measures taken by Boeing to improve the safety of pylon-to-wing connections are also mentioned [20].

1.4.5 Effect of countersink edge corrosion on fatigue crack initiation (W. 't Hart, NLR)

To investigate the effect of countersink edge corrosion on fatigue crack initiation a flight simulation fatigue test programme was performed on F-16 lower wing skin joint specimens. The specimen material was 7475-T7351, corresponding to the F-16 lower wing skin material. A low load transfer specimen type, called a Double Dogbone specimen, containing two 1/4 inch blind countersunk fastener was used, see figure 1. The specimen thickness were 9.6 and 6.3 mm corresponding approximately to the BL71 and BL110 locations of the F-16 wing. Before the specimens were assembled the countersink edges were pre-corroded in a corrosive solution resulting in corrosion depths of 0.2 to 0.5 mm. Subsequently the fatigue lives were determined for corroded specimens and specimens that received a corrosion removal treatment. Uncorroded specimens were tested as a reference.

For the fatigue tests the wing root spectrum "Basic" was used, representative for the average Leeuwarden AFB usage. The maximum stress in the wing root area is 213.74 MPa. However, for fatigue testing higher maximum spectrum stresses (110-120 %) were applied to obtain more realistic fatigue lives for uncorroded specimens and to limit the testing times. All the stress levels in the manoeuvre spectrum were scaled to the higher maximum stress levels.

It can be seen from figure 7 that for the 6.3 mm thick material a significant reduction in fatigue life was obtained with increasing corrosion depth. For the 9.6 mm thick specimens there was no evident effect of corrosion attack. The fracture surfaces after fatigue testing showed that fatigue crack initiation in the 6.3 mm thick specimens occurred on the corroded countersink edge (Fig. 8). This specimen type was considered in evaluating the effectiveness of corrosion removal on fatigue life.

Despite corrosion removal by Al_2O_3 grit blasting no improvement in fatigue life was observed. A cross-section over the treated countersink edge showed that the corrosion was not sufficiently removed and this explains why there was no positive effect of corrosion removal on fatigue life [21, 22].

1.4.6 Cadmium substitution in aircraft (W. 't Hart, NLR)

A Garteur (Group for Aeronautical Research and Technology in Europe) cooperation programme has been initiated to evaluate alternatives for cadmium plating for the corrosion protection of high strength steel aerospace components and fasteners. The selected alternative coatings were e.g. electro-deposited ZnNi and ZnCoFe, metallic ceramic deposits containing Zn and Al flakes and vapour deposited Al.

One aspect of investigation was the effect of coatings on fatigue life. Surface treatments such as pickling, anodising and plating may have a detrimental effect on fatigue life. Constant amplitude fatigue tests were performed on coated specimens from AIS/4340 steel heat treated to a tensile strength of 1400 MPa. Smooth and notched specimens with stress concentration values of $K_t = 1.4, 2.5$ and 4 were tested at a stress ratio of 0.1.

Fatigue testing was executed at British Aerospace, SAAB and the NLR. Bare and cadmium plated specimens were tested as a reference. All the electro deposited coatings received a baking treatment. An overview of available NLR test results is given in figure 9.

Note that for the ZnNi coating a significant reduction in fatigue strength is obtained. Although there is also an effect

for the ZnCoFe coating, the detrimental effect is not worse than for cadmium plating [23].

1.4.7 Three dimensional finite element analysis of three rivet row lap splice joint (S. Fawaz, TU Delft, A.U. de Koning, NLR)

A quarter of the FE model is shown in figure 10. It is composed of 1764 20 noded, isoparametric solid elements for both sheets and pins, while 364 non-linear gap elements define the interaction between sheets and pins. Both sheet and pins are assumed to be 2024-T3. The MSC/PATRAN pre/post processor is used, and the MARC finite element analysis program for solving the model. Two cases are considered, one representing a low squeeze force (LSF), and the other one a high squeeze force (HSF). In the latter case there are two stress systems, (i) the remote stress system, and (ii) a residual stress system created by rivet squeezing. The residual stress system represents the residual stresses created by expanding the rivet in the hole during rivet squeezing.

The most important result so far is the reduction of the cyclic stress by a factor of 3.2 as a result of the residual stress system in the HSF analysis. Due to rivet tilting in the LSF case, the rivet is losing contact with the bore of the hole at the net section of the joint, thereby moving the point of maximum stress away from the net section. In the HSF case, the rivet tilting is restricted due to the residual stress system. Additional analyses are underway with the inclusion of a quarter circular corner crack. More information on this topic is given in a paper at the Symposium.

1.4.8 Fatigue of riveted 2024-T3 and GLARE lap joints (R.P.G. Müller, TU Delft)

Research of R.P.G. Müller described in the previous review was documented as a Ph.D.-thesis [24]. It included both experimental and an analytical research on the fatigue behaviour of fuselage riveted lap joints. The most important outcome of the research is that the rivet squeeze force has a dominant effect on the crack initiation life of riveted joints. Therefore the squeeze force (and not the diameter of the driven head or the stroke during squeezing) should be carefully controlled during production. The squeeze force has two effects: (i) On the residual stress distribution around the rivet hole and (ii) on the geometrical imperfections of the sheet around the rivet holes which will have a large influence on the load transfer as well as the secondary bending of the sheet in this area. Imperfection may lead to *crack initiation in the nominally less critical bottom row*, which is not visible at the outside of the fuselage. Glare shows a similar response to the riveting parameters as 2024-T3, however, the fatigue life is much longer and crack growth is very slow, even at a high stress level. As an illustration figure 11 shows crack growth in the three thin 2024-T3 layers. Cracks first grow in the faying surface layer of the lap joint. After some 600.000 cycles cracks penetrate into the second layer. At that moment there is still a marginal loss of static strength.

1.5 FULL SCALE FATIGUE TESTS

1.5.1 Fokker 100 horizontal stabilizer-fin tear down inspection (H. Vlieger, NLR)

After having completed the whole fatigue/damage tolerance testing programme on the Fokker 100 horizontal stabilizer-fin test article with the execution of residual strength tests (performed in October 1994), on the test article a tear down inspection was carried out. Because the fin of this test article in combination with the test rig was planned to be used again, namely for mounting and testing of a composite horizontal stabilizer test box, prior to starting up of this test the damaged fin had to be repaired and a number of severely damaged parts of it had to be replaced. The repair of the fin was carried out by Fokker Aircraft Services (FAS) at their facilities at Woensdrecht. As a consequence of this repair/replacement a large number of damaged components of the fin became available for a tear down inspection. The released parts were transported to NLR in the Noordoostpolder, allowing there a detailed inspection of these parts. Further, of the 47 % main hinge fitting of the horizontal stabilizer (see Fig. 12) the LH part was removed completely from the test article for a tear down inspection while the RH part of it was inspected in situ.

Table 1 gives a survey of the results of the tear down inspection of components of the Fokker 100 fin in which already cracks were found during execution of the fatigue test (cracks found in other components are negligible). In these elements a number of new cracks was found. Almost all these cracks could not be found at the inspections carried out during the test either because they were hidden from observation owing to the presence of modification/repair elements applied during the test or owing to a poor accessibility for inspection. Further, in a number of cases the tear down inspection provided some supplementary and/or corrective information to that obtained from the fatigue test. Finally,

in the back-up structure of the main hinge fittings some new cracks were found in the angle profiles connecting these fittings to the surrounding structure.

1.5.2 Fokker 100 wing/fuselage damage tolerance test (S.J.W. Rutten, Fokker Services)

The fatigue and damage tolerance testing has been completed in 1994. It was followed by a residual strength test programme. The results have been reported at the ICAF-95 in Melbourne.

In 1995, 28 parts of the test article have been removed for tear down studies. Selection criteria for the tear down programme were:

1. Parts that were not tested long enough. Usually the required test factor on life was two. Some parts were changed or repaired during the test however and a test factor of two was therefor not achieved.
2. Locations that may exhibit multi-site damage problems (e.g. fuselage longitudinal and circumferential joints and wing cordwise splices).
3. Components with important cracks of which the crack growth rates could not be monitored during testing (e.g. the wing rear spar root end fitting).

The parts were disassembled in the Fokker Aircraft test department for visual inspection (approximately 15 areas). Other parts were sent to the materials investigation laboratory of Fokker and Shorts Bombardier. By means of Scanning Electron Microscope and Transmission Electron Microscope investigations, the initiation locations and crack growth rates were established. Until the bankruptcy of Fokker Aircraft (FAC) in march 1996, seven out of the twelve planned fractographic investigations had been finished. The remaining five parts are stored at the moment.

With the results, the inspection programme for the Fokker 100 will be completed. This work will be finished by Fokker Services which took over the Type Certificates for Fokker aircraft after the bankruptcy.

In the investigations numerous small defects were discovered that were not found during testing, ranging in size from 0.1 mm to 20 mm. The cracks had not affected the residual strength as was demonstrated by the preceding residual strength test programme. They may however indicate restrictions to load or life increase of the structure.

1.5.3 Fokker 60 fatigue and damage tolerance component tests (N.J. Fraterman, Fokker Aerostructures)

The Fokker 60 is a derivative of the Fokker 50 propjet ; the major changes are a stretched fuselage, higher design weights, an increased cruise speed and a large cargo door (3 * 2 meter) in the forward fuselage. Due to these modifications the fatigue spectra have change to such an extend that additional fatigue and damage tolerance tests were require for the certification of the Fokker 60 according to JAR 25.

The airworthness authorities required additional fatiguetests for areas, which were subjected to considerable higher fatigue loads than the Fokker 50, areas with newly designed structures and areas where the original Fokker 50 tests could not be extrapolated any further. The resulting testprogram consisted of a stress verification test on a prototype, component tests on the wing-fuselage connection, component tests on two locations in the outerwing and a component test of part of the large cargodoor plus surround. One test was executed by the NLR laboratory, while all the other tests were executed at the testdepartment of Fokker Aircraft in Amsterdam.

In order to verify the FEM stress-distribution, which is used for the definition of the test spectrum, a stress verification test has been performed on one of the prototypes. During this test cabin pressure, up/down fuselage bending and a drag load on the main landinggear, simulating braking, has been applied. Stresses have been measured at the wing-fuselage connection, the large cargodoor surrounding and the large cargodoor supports. The results have been used for fine-tuning the FEM stress-distribution and the testspectra.

The tests on the wing-fuselage connection consisted of a component test of the wingside and an other component test on the fuselage side, see figure 13. The test spectrum consists of flightloads due to gust/manoeuvre plus cabin-pressure and groundloads due to taxi, turning, landing-impact and braking. The wing-fuselage connection had been designed and certified as a slow crack growth structure. Therefore the components will be tested for at least two life times (180000 fc); thereafter artificial cracks of 0.05" will be inflicted at the critical locations and the tests will continue



for an other two lifetimes (180000 fc). So the wing fuselage connection will be tested for a total of four lifetimes (360000 fc). The test on the wingside component has successfully been completed, whereas the fuselage component has reached 125000 fc without any damage in the test area and will continue till the end of 1997.

One of the wing components consisted of bonded stringer run-outs in the lower wing skin near a flap support rib. The testspectrum contains flightloads due to gust/manoeuvre and ground loads due to taxi/landing. This area is designed and certified as a multi-loadpath structure and will therefore be tested for two and a half lifetimes (235000 fc) of which the last half will be run with artificial cracks. Cracks have been found after 70000 fc at the end of the bonded skinflange of the stringer and were caused by the unfavorable ratio of stringerflange to skin-thickness. The crackgrowth was monitored up to 100000 fc and subsequently a repair was performed at the crackareas. The test was than continued and has reached 182000 fc in march 1997.

The other wing component represents a fatigue critical splice in the lowerskin of the outer wing. The testspectrum contains flightloads due to gust/manoeuvre and groundloads due to taxi/landing. The design and certification philosophy of this area is identical to the other wingcomponent and will also be tested for a total of 235000 fc. This test has just been started and will continue till the end of 1997.

The large cargo door component represent the critical locations of this door and its surround, including the pianohinge plus backup at the upperside and the hooks plus spoolbrackets and backup at the lowerside. The testspectrum consists of cabin pressure and shear across the door due to flight/ground loads. The door and its supports are designed as a multi load path structure and will be tested for two and a half lifetimes (235000 fc) of which the last half will be run with artificial cracks. Subsequently the test will be continued for 30000 fc with an increased spectrum in order to simulate the complete failure of a hook, so the test will run for a total of 265000 fc. Up to march 1997 the test has reached 150000 fc without any damage in the testarea and will continue till october 1997.

1.5.4 Gulfstream V horizontal stabilizer fatigue and damage tolerance test (J.E.A. Waleson, A. Buitenhuis, Fokker Aerostructures)

The Gulfstream V horizontal stabilizer and vertical fin have been designed and are built by Fokker Aerostructures. The fatigue and damage tolerance test on the metal structure of the horizontal stabilizer and the pivot fitting area, which connects it to the vertical fin, are conducted at Schiphol. The static test article of the vertical fin is used as dummy structure to ensure a proper load distribution at the interface. However, all parts of this static test article at the pivot fitting area, including the rear beam and the top rib, have been replaced and are part of the test.

The test duration for the total structure amounts to two life-times (2*16,000 flights) minimum. Extra flights, up to half a lifetime, are scheduled for damage tolerance testing with one load path of multi-element structure completely severed. Further, an extra 32,000 flights with cycles which are critical for the pivot fitting only (asymmetric cycles) have been added. Thus, the pivot fitting can be fatigue tested for four lifetimes in total.

Up to date the total structure has been tested for 18,000 flights. The fatigue test on the pivot fitting has covered 50,000 flights. No natural cracks have occurred. One 0.05" crack in the pivot fitting inflicted by means of spark erosion has been present from the beginning of the test. No growth has been found.

Fatigue and damage tolerance tests on the CFRP elevator (full scale test) and trimtab (subcomponent test) have been carried out in separate test set-ups. In the elevator test, the position of three of the five hinges was adjustable (displacement-controlled) in order to represent forced deflection of the stabilizer. CFRP parts and metal parts have been tested simultaneously. A load enhancement factor of 1.13 in combination with a scatter factor of 2 have been used for this purpose (conservative for the metal parts).

Level 1 damage in CFRP parts (barely visible impact damage and delaminations) and level 2 damage in metal parts (0.05" cracks by spark erosion) have been present from the beginning of the test. After completion of the second life, some damage tolerance conditions have been tested during a third life: a hinge failure, missing fasteners, and clearly visible impact damage. Fatigue cycling of these damage tolerance conditions is important since it could take some time



until such a damage is detected in service. Three inspection intervals have been tested for each condition to account for missing it twice during scheduled maintenance.

After 48,000 flights, the only fatigue damage found was small growth from an artificial damage in one of the metal hinge swivels (single load path slow crack growth). For the CFRP parts, none of the damages showed any growth. The same test articles have been used for static testing after completion of the fatigue and damage tolerance tests. Ultimate load capability has been shown in these static tests.

1.5.5 Full scale fuselage panel tests (R.W.A. Vercammen, NLR)

In service fuselages are subjected to cabin pressure and fuselage bending. Therefore it is highly desirable that in case of fuselage design studies curved structures are tested under these biaxial loading conditions. For this purpose barrel test set-ups are generally used. These set-ups, however, are less attractive for studies not directly related to a particular aircraft design: the radius of curvature is fixed, a large number of panels has to be tested simultaneously and the test frequency is rather low. In addition, barrel tests are expensive due to the large number of panels and long testing times. The panel test facility at NLR was developed to avoid these disadvantages [25]. In this facility, which is flexible in panel diameter (ranging from small aircraft like the Fokker 50 to large aircraft like the Airbus A300), panel width and panel length, a single fuselage panel can be tested in a relatively short time.

In the framework of the Brite Euram IMT 2040 programme "Fibre reinforced metal laminates and CFRP fuselage concepts" Fokker Aircraft designed and built a GLARE fuselage panel. The panel was representative of the crown section of the Fokker 100 fuselage, just in front of the wing. The panel (1210 mm * 3030 mm) had a skin made of GLARE A¹ and contained seven GLARE N² stringers, five aluminium frames, stringers couplings, rigid stringer-frame attachments and a longitudinal riveted lap-joint in the panel centre. A complete Fokker 100 crown section made of GLARE A with GLARE N stringers and rigid stringer-frame attachments would have a weight that is 63 % of the current design in aluminium.

Under contract to Fokker, NLR tested this GLARE panel. The panel was subjected to circumferential loads caused by internal air pressure and axial loads, representative of both cabin pressure and fuselage bending due to taxiing and gust loading.

A fatigue test was performed in which 180,000 flights (two lifetimes) were simulated. The load sequences of the fatigue spectrum were derived from the Fokker 100 full-scale test. The testing frequency was about 10,000 flights per 24 hours. After the fatigue test no damage was observed. The fatigue test was followed by static tests to Limit and Ultimate Load. Finally the panel was loaded to failure at 1.32 * Ultimate Load [26], [27].

The results of the GLARE fuselage panel tests proved that the use of GLARE leads to a substantial weight reduction without affecting the fatigue or static strength. The new full-scale fuselage panel test facility has shown to operate correctly. The load introduction in the panel in axial and circumferential direction was uniform and realistic fatigue loads due to cabin pressure and fuselage bending could be applied at high frequency.

In the framework of the Brite Euram programmes "Advanced concept for large primary metallic aircraft structures" and "Structural maintenance of ageing aircraft" NLR will test several fuselage panels of Shorts, DASA and Alenia.

¹ GLARE A = GLARE 3-2/1-0.3 = 2 * (0.3 mm 2024 sheet) + (0.25 mm cross-ply glass prepreg).

² GLARE N = GLARE 1-3/2-0.3 = 3 * (0.3 mm 7475 sheet) + 2 * (0.25 mm UD glass prepreg).

1.5.6 Testing the centre section of a composite stabilizer (H.G.S.J. Thuis, NLR)

As part of a composite stabilizer technology program a number of static and fatigue tests will be carried out on the "4-meterbox": a structurally complete composite centre section of a stabilizer for the F28 Mk0100 jetline (see Fig. 14). The purpose of the test program is to verify:

- a. The elastodynamic behaviour of the "4-meterbox" as determined by analysis.
- b. The strain distributions in the "4-meterbox" as determined by analysis.
- c. The "no-growth concept" of the "4-meterbox" during fatigue loading.

- d. The strength of the "4-meterbox" up to Ultimate Load (UL) with Barely Visible Impact Damages (BVID).
- e. The damage tolerance behaviour of the "4-meterbox".

During these tests the "4-meterbox" will be attached to a metal full size vertical stabilizer. The vertical stabilizer itself will be connected to a rigid test frame (see Fig. 15). A number of hydraulic actuators (ten for the static tests and twelve for the fatigue tests) will be used to introduce the required loads to the "4-meterbox". The loads will be introduced via two elevator supports, six stainless steel clamps and two stainless steel dummy outboard sections (see Fig. 16).

The overall test program will contain a number of static tests at elevated temperature and high relative humidity. During these tests the "4-meterbox" will be positioned in an environmental chamber (7 m x 3 m x 2.5 m see Fig. 17). The overall test program (subjected to only one "4-meterbox") contains the following tests:

Test no. 1: Elastodynamic test.

Test no. 2: Static strain survey to Limit Load.

The test will be carried out at ambient conditions.

After test no. 2 the "4-meterbox" will be saturated in the environmental chamber. During saturation the temperature in the environmental chamber will be 80 °C and the relative humidity 85 %. When the "4-meterbox" is fully saturated the test program will be continued as follows:

Test no. 3: Fatigue test.

The test will be performed at room temperature with the "4-meterbox" in aged condition. An equivalent of 90.000 flights (1 x the life of the aircraft) will be tested with a load enhancement factor of 1.18. Since composites are considered not to be sensitive to low amplitude fatigue loads the number of cycles per flight were reduced considerably by deleting all cycles which introduce strain levels of 500 micro strain or less to the "4-meterbox" from the fatigue spectrum. This resulted in a reduced fatigue program with an average of 2.5 cycles per flight.

When the fatigue test has been completed the "4-meterbox" will be subjected to a number of static tests. It was decided to carry out these tests at elevated temperature (80 °C) and increased humidity (85 % R.H) in stead of using an environmental knock-down factor. Therefore after test no. 3 the "4-meterbox" will be saturated again and the test program will continue with the following tests:

Test no. 4: Static Ultimate Load test with BVID's in the "4-meterbox".

Test no. 5: Static Limit load test with Visible Impact Damages in the "4-meterbox".

Test no. 6: Static "Get Home" load test (70 % Limit Load for manoeuvre load cases and gust cases with 40 % Limit gust velocity) with a simulated failed front spar.

Test no. 7: Static Limit Load test with repaired front spar.

Test no. 8: Static test to failure.

At this moment test 1: aeroelastic test and test 2: static strain survey to Limit Load have been carried out successfully. The "4-meterbox" is now being saturated in the environmental chamber.

1.5.7 Definition of gust test load conditions for fatigue tests (J.B. de Jonge, W.J. Vink, NLR)

A fully automated procedure has been developed for the generation of gust test load condition sequences to be applied in full scale fatigue tests. The procedure uses a continuous or so-called PSD-gust concept. A PSD-gust model, based on the most recent gust statistical data (Ref. 28) is defined and proposed for application, see table 2 and figure 18. The incremental load distributions associated with the gust load test conditions are defined in such a way that in each section one specific load quantity, e.g. the lower wing skin stress, which is considered as the "most significant" with regard to fatigue is simulated properly. This load quantity is indicated as "master load". The master load assumes its proper value when the sectional loads (M,T,S) have the "correlated" value. This correlated value of a sectional load is the "most probable" value for that sectional load, under the condition that the master load has its desired value [29].

1.6 AGEING AIRCRAFT

1.6.1 Structural Maintenance of Ageing Aircraft (SMAAC) (W.J. van der Hoeven, NLR)

The NLR participates in the Brite Euram programme "Structural Maintenance of Ageing Aircraft (SMAAC)". The programme started in 1996 and is sponsored by the Commission of the European Communities. The activities of the NLR are:

1. To evaluate the extent of multiple site damage by studying the fracture surfaces of in-service MSD failures. One of the samples to be analysed is a section of a longitudinal lap joint of an aged BAC1-11 aircraft which was supplied by British Aerospace. The investigation carried out so far indicated that there were some very small fatigue cracks in some sections of the joint. In addition, F28 lap joints samples that contain multiple cracks at rivet holes will be analysed.
2. In the field of model development there are three activities:
 - Modified in-house NLR software was used to predict the residual strength of aluminium alloy sheets with several collinear cracks. The predictions were in good agreement with experimental results. During the SMAAC programme the software will be extended to make it suited for predictions of stiffened structures with MSD.
 - A 3-D FEM model of a riveted lap joint with 3 rivet rows was made (the width of the model was 1 rivet pitch). Using the model it was shown that the degree of rivet interference had a large effect on the stress intensity factor for cracks emanating from the rivet holes.
 - The NLR is studying the applicability of existing software (based on Monte-Carlo simulation model) to predict the development of MSD in typical aircraft structures. Using the software the inspection interval and threshold will be calculated. The results will be compared with the inspection intervals predicted for single site damage growth. In addition, all partners will participate in a numerical round robin programme to evaluate in house programmes. If necessary the NLR software will be modified.

Finally, there are several NLR contributions which are planned for the second and third year of the SMAAC programme, but which have not started, such as:

- To perform tests on full scale fuselage panels with MSD. The curved fuselage panels (about 3 m in length and 1.5 m in width) will be tested in the recently developed test rig. The panels will be supplied by Deutsche Aerospace Airbus and by Alenia.
- Fracture surfaces of fatigue tested lap joint specimens will be analysed to study the initial stages of fatigue crack growth (locations of crack initiations, crack growth rates and development of crack shapes).
- Fatigue tests will be done on pre-corroded lap joint specimens. The conditions during pre-corrosion will be chosen such that the resulting corrosion damage is representative for corrosion observed under in service conditions. The results will be used to develop a methodology, based on the damage tolerance approach, that takes account of environmental and time effects.

1.6.2 Corrosion Fatigue (R.J.H. Wanhill, NLR)

A review was made of the problems of corrosion and fatigue in ageing aircraft, concentrating on fuselage longitudinal lap splices owing to the current concern about Multiple Site Damage (MSD). It is often assumed that interactions between corrosion and fatigue will occur, but is it actually unknown whether in-service corrosion habitually leads to fatigue cracking (except in the case of "star cracks" around rivet holes where massive corrosion has occurred) and to what extent the service environment affects fatigue crack growth. There is a need to investigate the relations between fatigue and corrosion in ageing aircraft, as is currently being done in Canada and Europe for civil aircraft and by the USAF, and to do realistic environmentally-influenced fatigue tests. These tasks are essential for developing fatigue analyses that account for in-service corrosion, if necessary, and the environment conditions of crack growth.

Ref.: NLR Technical Publication TP 96253, "Some Practical Considerations for Fatigue and Corrosion Damage Assessment of Ageing Aircraft", Revised Version to be issued in 1997.

1.6.3 Residual strength tests on stiffened panels with multiple cracks (H.J. ten Hoeve, NLR)

At different institutes and in industry software for the prediction of the residual strength of panels with multiple site damage (MSD) is developed or under development.

In most cases this software does not model the lap joint but only the cracks. The influence of secondary bending and the stresses introduced by the riveting process are not taken into account. To be able to verify these models tests are done on stiffened panels with multiple cracks but without lap joint. These test panels are closest to the models developed. All panels tested had a width of 1190 mm six tests were carried out on panels with four stiffeners. From these tests four formed a series of a 120 mm lead crack and different combinations of MSD cracks. In addition five tests were carried out on panels with three stiffeners. This includes one test with a single crack and an intact central stiffener and four tests with a broken central stiffener. From these test three formed a serie with a lead crack of 160 mm and different combinations of MSD cracks [31].

1.6.4 Prediction of residual strength in panels with multiple collinear cracks (H.J. ten Hoeve, NLR)

Under contract with ESA, NLR implemented a Strip Yield model in the NASA crack growth calculation program NASGRO. This Strip Yield model is based on the Dugdale and Barenblatt model and predicts crack growth retardation and acceleration due to plastic deformations near the crack tip. This Strip Yield model can also be used to calculate the crack tip opening displacement and plastic deformations for a series of collinear cracks. From the crack tip opening displacement of all tips the residual strength can be calculated using an R-curve or Kc approach. The plastic deformations can again be used to predict the plasticity induced retardation and acceleration for MSD cracks [32].

1.7 FIBER METAL LAMINATES

1.7.1 The damage tolerance behaviour of riveted GLARE3-3/2-0.2 lap joints, (W. van der Hoeven, NLR)

The damage tolerance behaviour of a riveted GLARE3-3/2-0.2 single lap joint was investigated and the potential of this material as skin for aircraft fuselages was evaluated.

GLARE3-3/2-0.2 is one particular grade of Fibre Metal Laminates. It consists of three 0.2 mm thick Al2024 T3 layers that are bonded together with a glass fibre reinforced structural adhesive. The glass reinforcement is in two mutual perpendicular directions.

The riveting force used in producing the single lap joint test specimens was the main variable in the testing programme. The applied riveting force can be characterized by the ratio of formed head diameter to rivet diameter. Lap joint specimens with three different D_d/D ratios were prepared: $D_d/D = 1.25$, 1.35 and 1.6. The ratio $D_d/D = 1.25$ is the smallest allowable ratio at Fokker Aircraft. For each specimen the D_d/D ratio was the same for all rivets. The lap joint specimens, representing a longitudinal fuselage skin joint, were fatigue tested to a predetermined number of constant amplitude fatigue cycles. After the fatigue tests the fatigue damage in the specimens was determined with a more or less standard eddy current inspection method. Subsequently, the specimens were statically loaded to failure to determine the residual strength.

Increasing the riveting force was shown to have a beneficial effect on both the fatigue and residual strength behaviour of the joint. The effect of fatigue life on the residual strength of the joint is illustrated in figure 19. As can be seen, when using a relative high D_d/D ratio of 1.6 the residual strength hardly decreases during as much as 10^6 cycles (each cycle represents one flight). Specimens fatigue tested to 10^6 cycles had fatigue cracks at most of the rivets in the critical rivet rows. However, the cracks were in the adjacent aluminium face sheets of the laminates only.

The performance of the applied eddy current inspection method was evaluated by comparing all crack length data measured with this inspection method with those measured visually. The accuracy of the method for cracks in the mating aluminium layers of the riveted GLARE3 sheets was about 2 mm and the minimum detectable crack length was estimated to be about 3 - 4 mm [33].

1.7.2 Repair with bonded fibre metal laminate patches (A. Vlot, TU Delft)

This joint research programme with the United States Air Force Academy aims at soft patching, i.e., the bonding of patches of strong, moderate modulus repair material on aircraft. Further development of the CalcuRep design tool took place, including the refinement of the analysis of tapered patches and the secondary bending at the patch tip. This bending is very important because it may cause crack initiation in the aluminium fuselage skin if the design is inaccurate. CalcuRep was verified with FE-calculation and strain measurements. The thermal stresses around a hot bonded repair on a Fokker F-28 fuselage section were determined. This revealed thermal buckling problems at too high curing temperatures. Fatigue tests were done to compare the effectiveness of GLARE and boron/epoxy patches. Glare proved to be superior. Also the effect of debonds, simulating bad bonding procedures, were checked. Two bonded Glare patches were installed on a C5-A Galaxy and will be inspected regularly.

1.7.3 Stable static crack growth in GLARE, R-curves (C. Vermeeren, TU Delft)

Stable crack extension under a statically increasing load was studied by Coen Vermeeren [34] by testing sheet specimens of GLARE fiber-metal laminates with a width up to 800 mm. Extensive stable crack extension was observed, while some delamination occurred in the plastic zone of the growing cracks in the Al lamina. Stable static crack extension in GLARE is controlled by fiber failure. Large plastic zones can develop in the Al-alloy lamina, while the fibers are still elastic. As a consequence, the classical evaluation of R-curves from the test results appears to be questionable. The experiments have also shown that prevention of crack edge buckling leads to a higher crack growth resistance. However, it is difficult to prevent out-of-plane displacements near the crack tip. In view of this observation, there is still a relevant question with respect to the restraint on such displacements in a pressurized fuselage.

1.7.4 Spliced Fibre Metal Laminates (T.J. de Vries and A. Vlot, TU Delft)

The maximum sheet width for 0.3 mm thick aluminium, and thus for GLARE laminates with this type of aluminum layers, is approximately 1.65 m. However, for the purpose of skin material in a fuselage, wider sheets are preferred to reduce the amount of necessary joints. This problem can be solved with the splicing concept; metal sheets are interrupted in the laminate and these splices are bridged by the fiber layers, see figure 20. With this concept the sheet width can be increased to 4 meters or more, depending on the autoclave size. Using these large sheet sizes can provide an additional weight and cost saving compared to monolithic aluminum structures due to a reduction of the number of riveted joints.

Fatigue and static strength tests on spliced laminates with varying fibre orientation were performed to determine design allowables. Residual strength tests on spliced laminates with through cracks showed that the splices can effectively stop stable crack extension. In this case the crack has to reinitiate at the other side of the splice.

1.7.5 Fatigue tests on small fiber-metal laminates specimens (J. Schijve, TU Delft)

In this investigation, which is carried out in cooperation with the Institute of Metal Physics of the University of Agriculture, Vienna, small fiber-metal laminates specimens (width 12 mm) were tested at a very high frequency of 20 kHz at $R = -1$ (ultrasonic test set-up).

In one investigation specimens of GLARE 1 (7475-T76 lamina, poststretched) were provided with a small edge notch (depth 2 mm, specimen width 12 mm) and root radii of 1, 2, 4 and 8 mm, corresponding to K_t values of 4.3, 3.4, 2.7 and 2.0 respectively. Two stress amplitudes were used (70 and 100 MPa). Crack initiation and propagation were observed with optical microscopes and two video camera's (160 x). Results of the crack initiation life plotted as a function of the amplitude of the peak stress at the notch root were obtained in a single scatter band for all tests (Wöhler curve). The crack initiation life was obtained by extrapolating the crack growth curve to zero crack length. Crack growth rates were lower for the smaller K_t values. The growth rate showed the characteristic behaviour of poststretched fiber-metal laminates, i.e. a significantly decreasing growth rate until very low values. Illustrative results are shown in figure 21. More results are presented in [35], also on the location of the microcracks along the root of the notch.

In another investigation ARALL 2 and GLARE 2 specimens were tested, both fiber-metal laminates with a 3/2 lay-up, three 2024-T3 lamina (0.3 mm) and two prepreg layers with aramid or glass fibers respectively. Poststretching is not applied to these laminates. Crack growth initiated by a sharp notch was significantly delayed by the fibers, but not



in the same way in the two fiber-metal laminates. At a low stress amplitude the results were similar, but for higher amplitudes GLARE 2 was considerably superior. This could be explained by fiber failure occurring in the ARALL specimens, whereas it did not occur in the GLARE specimens, even at high stress amplitudes. The results were evaluated in terms of an empirical K_{bridging} associated with crack bridging of the fibers [36].

1.7.6 Fatigue investigation of Structural Laminates Company, SLC (G. Roebroeks, SLC)

a Influence of the internal stress in GLARE[®] 1, on the fatigue behaviour

The fatigue behaviour of unstretched GLARE[®] 1, based on 7475-T761 aluminum sheet is relatively poor compared to that of the other 2024-T3 based GLARE[®] materials. To overcome this problem GLARE[®] is post stretched, reversing the internal stress in the layers of the material: compression in the aluminum layers and tension in the fiber layers. It considerably improves the fatigue properties. There are two possibilities to define the stretching operation:

- Stretching to a constant permanent strain.
- Stretching to a constant internal stress.

The first procedure is based on a more simple definition. However, the second one leads to more uniform properties for different lay-ups. Fatigue crack growth results on this question are presented in [37].

b Environmental effects on the fatigue behaviour of GLARE[®]

If there is an environmental effect, a frequency effect should also be expected. Fatigue crack growth experiments were carried out at a frequency as low as 0.0033 Hz (one cycle in 5 minutes). The effect of moisture was also investigated. It turned out that the load frequency and the humidity have a rather small influence on the fatigue crack growth rates [38].

The effect of the environment on the behaviour of riveted lap joints was investigated with tests in distilled water and salt water immersion in order to study the fatigue behaviour and residual strength after fatigue. Tests on 2024-T3 lap joints were carried out as base line data. Environmental effects were observed indeed. However, in each environment the GLARE[®] lap joints showed a similar superiority if compared to the behaviour of 2024-T3 lap joints. It appears that the environmental effects are related to effects on the aluminium layers, but the advantage of the fiber-metal laminates concept is maintained [38].

c Thermal behaviour of GLARE[®]

Various aspects of the thermal behaviour of GLARE[®] are investigated and reported in [39]:

- Thermal conductivity (through the thickness of the material).
- Thermal expansion.
- Thermal fatigue.

The thermal fatigue behaviour of GLARE[®] was studied by exposing the material to a cyclic temperature range from - 50 °C to + 80 °C, up to a maximum of 1000 cycles (one cycle in 46 minutes). The purpose of the tests was to see whether it might cause any physical damage or material degradation. In addition to two standard laminates (GLARE 2-3/2-0.3 and GLARE 3-3/2-0.2) two non-standard lay-ups were tested in order to get more excessive residual stresses in the metal and the layer after production. High residual stresses were introduced by post-stretching GLARE 3-3/2-0.2 to 0.6 %. High residual compressive stresses in the fibers were obtained by manufacturing GLARE 2-2/1 with two 2024-T3 layers of a large thickness (2.6 mm). After exposure to the thermal fatigue conditions, the specimen were investigated using the C-scan, the scanning electron microscope and ILSS tests. None of the investigations showed material degradation for any of the variables studied.

d Fatigue behaviour of spliced GLARE[®] configuration

A spliced GLARE[®] panel was developed for the A340. In 1995 the full analysis of the configuration was completed. The tests included tensile strength, residual strength, blunt notch, off-axis behaviour, shear buckling, riveting issues, quality but also fatigue crack initiation and growth. All results are compiled in [40].

An important type of cracking of GLARE[®] structures is fatigue crack initiation in an outer aluminum sheet of the laminate at the edge of a doubler. The splice configuration for the A340 side panel uses a GLARE[®] doubler bonded



over the splice to locally reduce the stress for preventing delamination initiated by the interrupted aluminum layers. The crack initiation behaviour at the doubler edge was evaluated in experiments. Also crack growth from large saw cuts (25 mm and 75 mm) at the doubler edge was studied.

The test results show that crack initiation did not occur for the thickness step used for the splice area. Damage was not found after 400,000 fatigue cycles from 6 to 120 MPa. Also the proposed doubler configuration around the windows in the GLARE[®] side panel did not cause crack initiation. The fatigue crack growth tests on configurations with saw cuts at the doubler edge showed lower crack growth rates than those found for the basic GLARE 3-3/2-0.3 skin material. The study showed that fatigue crack initiation and growth is not a critical aspect for the splicing geometry chosen for the A340 side panel.

e Fatigue crack growth prediction in GLARE[®]

The fatigue crack growth behaviour of Fiber Metal Laminates has been modelled by Marissen [41]. The calculation method uses crack growth data of the metal sheet in ARALL[®] or GLARE[®]. Because of the low K values due to crack bridging fibers, the relation between crack growth rate (da/dN) and the stress intensity factor should be available at these low K values for the thin aluminum sheet used in FML's to calculate the crack growth rates. This relation was believed not to be available with sufficient accuracy. A crack edge loading specimen was used to generate new crack growth data for the thin aluminum sheet in the required K range. These results were used in Marissen's model to calculate the fatigue crack growth behaviour in various GLARE[®] materials [42]. Reasonable correlation between prediction and measurement was found (Figs. 22a and 22b). Discrepancies can be associated with shortcomings of the prediction model.

1.8 REFERENCES

1. Jonge, J.B. de; Hol, P.A., "Variation in Load Factor Experience of Fokker F27 and F28 Operational Acceleration Exceedance Data." U.S. Department of transportation DOT/FAA/AR-96/114. (Also published as NLR Technical Publication TP 96512 U).
2. Gelder, P.A. van, "Fokker 100 Tail Load Measurements - Database description -", NLR CR 95618 L.
3. Gelder, P.A. van, "Analysis of Operational Tail Loads of a Fokker 100 Aircraft", NLR CR 96779 L.
4. Gelder, P.A. van, "Analysis of Measured In-Flight Tail Loads", NLR TP 96279 L, (presented at the 20th ICAS Congress, Sorrento (Italy), as paper ICAS 96-5.3.2).
5. Gelder, P.A. van, "Derivation of Lateral and Vertical Gust Statistics from In-Flight Measurements", NLR TP 97036 L, (presented at the 38th Structures, Structural Dynamics and Materials Conference, Kissimmee (FL), USA, as paper AIAA 97-1214).
6. Laméris, J., "Derivation of multiple linear regression equations between wing root loads and flight parameters for the TuAF F-16C," report CR 96503 L, National Aerospace Laboratory-NLR, August 1996.
7. Laméris, J.; Pho, J.C.C., "Derivation of multiple linear regression equations between wing root loads and strain gauge response for the TuAF F-16C", report CR 95294 L, National Aerospace Laboratory-NLR, June 1996.
8. Dominicus, J.A.J.A., "A-7P revised test programme results within PoAF DDI Project phase II" NLR CR 97108 L, 1997.
9. Dominicus, J.A.J.A., "Damage Tolerance of Plate Structure to finalize A-7P activities within PoAF DDI Project Phase II", NLR CR 97xxx L, to be issued.
10. Koning, A.U. de; Hendriksen, T.K., "Damage tolerance analyses of bolt/nut assemblies." Proceedings of ECFH Conference. ed. J. Petit: "Mechanisms and mechanics of damage and failure", Vol. 1, pp. 335, Poitiers, 1996.
11. Koning, A.U. de; Lof, C.J.; Schra, L., "Assessment of 3D Stress intensity factor distributions for nut supported threaded rods and bolt/nut assemblies". ESA Contract Report NLR CR 96692 L, 1996.
12. Fawaz, S., "Application of the virtual crack closure technique to calculate stress intensity factors for through cracks with an oblique elliptical crack front". Report LR-805, Delft Un. of Tech., Fac. of Aerospace Eng., Sep. 1996.
13. Koning, A.U. de, "Dynamically loaded aerospace structures". NIVR Contract Report NLR CR97xxx L, 1997, to appear shortly.
14. Hoeve, H.J. ten; Koning, A.U. de, "Architecture and detail design of the STRIPY NTV 1.0 strip yield module in the NASGRO or ESACRACK software", ESA Contract report NLR CR 96506 L, 1996.

15. Wanhill, R.J.H.; Boogers, J.A.M.; Kolkman, H.J., "Completing NLR contributions to the IEPG TA 31 programme", Parts I-IV; NLR CR 97035 L; National Aerospace Laboratory NLR, Amsterdam, February/March 1997.
16. Schijve, J., "Fatigue crack growth under variable-amplitude loading". Fatigue and Fracture, American Society for Materials, Handbook Vol. 19, ASM, 1996, 110-133.
17. Schijve, J., "Predictions on fatigue life and crack growth as an engineering problem". A state of the art survey. Fatigue 96, Berlin, Proceedings 6th International Fatigue Congress, Vol. II, pp. 1149-1146. Eds. G. Lütjering and H. Nowack, Pergamon 1996.
18. Laméris, J.; Schra, L., "Applicability of the crack severity index (CSI) for fatigue crack initiation," report CR 96061 L, National Aerospace Laboratory-NLR, January 1996.
19. Wanhill, R.J.H., "Damage Tolerance Engineering Property Evaluations of Aerospace Aluminium Alloys with Emphasis on Fatigue Crack Growth", NLR TP 94177 U.
20. Wanhill, R.J.H.; Oldersma, A., "Fatigue and fracture in an aircraft engine pylon", NLR TP 96719 U.
21. Hart, W.G.J. 't; Boogers, J.A.M., "Effect of countersink edge corrosion on fatigue crack initiation", NLR CR 94114 L.
22. Hart, W.G.J. 't; Boogers, J.A.M., "Fatigue tests on corroded simulated F-16 lower wing skin joints", NLR CR 95492 L.
23. Various Authors, "Environmentally Compliant Surface Treatments of Materials for Aerospace Applications". Paper presented at AGARD SMP Meeting, Florence September 1996.
24. R.P.G. Müller, "An experimental and analytical investigation on the fatigue behaviour of fuselage riveted lap joints". The significance of the rivet squeeze force, and a comparison of 2024-T3 and Glare 3. Doctor thesis, Delft University of Technology, Oct. 1995.
25. Jong, G.T. de; Elbertsen, G.A.; Hersbach, H.J.C.; Hoeven, W. van der, "Development of a full-scale fuselage panel test methodology", NLR contract report CR 95361 C, May 1995.
26. Vercammen, R.W.A., Full-scale GLARE fuselage top-panel test, NLR contract report CR 96301 C, May 1996.
27. Vercammen, R.W.A.; Ottens, H.H., "Full-scale GLARE fuselage panel tests", NLR technical publication TP 96530 L, August 1996. Paper presented at the FAA-NASA Symposium on Continued Airworthiness of Aircraft Structures, August 28-30, 1996.
28. Jonge, J.B. de; Hol, P.A.; Gelder, P.A. van, "Reanalysis of European Flight Load Data". Federal Aviation Administration DOT/FAA/CT94/21, 1994.
29. Jonge, J.B. de; Vink, W.J., "Gust Load Conditions for Fatigue Tests based on a Continuous Gust Concept". Paper presented at 38th AIAA/ASME/ASCE/AHS/ASC meeting, Kissimmee Fl. April 1997, NLR TP 97015 U, 1997.
30. Wanhill, R.J.H., "Some practical considerations for Fatigue and Corrosion Damage Assessment of Ageing Aircraft", NLR TP 96253, revised version, to be issued in 1997.
31. Hoeve, H.J. ten; Schra, L.; Michielsen, A.L.P.J.; Vlioger, H., "Residual strength tests on stiffened panels with multiple site damage". NLR CR 96792 L.
32. Hoeve, H.J. ten; Koning, A.U. de., "Reference manual of the Strip Yield module in the NASGRO or ESACRACK software for the prediction of retarded crack growth and residual strength in metal materials", NLR CR 97012 L.
33. Hoeven, W. van der, "The damage tolerance behaviour of riveted GLARE3-3/2-0.2 lap joints. The effects of riveting force and fatigue stress level". NLR CR 96711 L.
34. Vermeeren, C.A.J.R., "The residual strength of fibre metal laminates". Doctor thesis, Delft University of Technology, Dec. 1995.
35. Papakyriacou, M.; Stanzl-Tschegg, S.E.; Schijve, J., "Fatigue behaviour of notched components of fiber-metal laminates (GLARE)". Fatigue Design 1995, Vol. 1, Ed. by G. Marquis and J. Solin. Technical Research Centre of Finland, Espoo 1995, 309-320.
36. Papakyriacou, M.; Schijve, J.; Stanzl-Tschegg, S.E., "Estimation of the fiber bridging capability of two fiber-metal laminates at high cycle fatigue loading". Fatigue 96, Berlin, Proceedings 6th International Fatigue Congress, Vol. III, pp. 1523-1528. Eds. G. Lütjering and H. Nowack, Pergamon 1996.
37. Verolme, J.L., "A study on the internal stress in GLARE 1". Report TD-R-95-025, Structural Laminates Company, 22 December 1995.
38. Roebroeks, G.H.J.J.; Müller, R., "Corrosion fatigue testing of aluminum and GLARE riveted lap joints". Report TD-R-95-010, Structural Laminates Company, 31 August 1995.
39. Verolme, J.L., "Thermal behaviour of Fiber Metal Laminates", Report TD-R-95-024, Structural Laminates Company, 24 January 1996.



40. Roebroeks, G.H.J.J., "The development of the splice geometry for the Daimler-Benz Aerospace Airbus GLARE 3-3/2-0.3 barrel test panel". Report TD-R-93-005B, Structural Laminates Company, 1 May 1995.
41. Marissen, R., "Fatigue crack growth in ARALL - a hybrid aluminum - aramid composite material, crack growth mechanisms and quantitative predictions of the crack growth rates. Ph.D. Thesis, Report LR-574, Faculty of Aerospace Engineering, Delft University of Technology, Delft, The Netherlands, 1988.
42. Verolme, J.L., "Prediction of constant amplitude fatigue crack-growth in Fiber Metal Laminates". Report TD-R-95-013, Structural Laminates Company, 2 October 1995.

Table 1 Survey of results of tear down inspection of Fokker 100 fin (see Fig. 12)

	Damage Report no.	Results of tear down inspection		
		Supplementary/corrective information with respect to that from test results	Type of inspection ^{*)}	New cracks found
RIB 5.0	4-88	yes/no	1	no
	4-89	no	1 + 2	no
	7-91	no	1	yes
	3-93	no	1	yes
	4-93	no	1	yes
	12-93	no/yes	1	yes
	13-93	no	1	yes
	4-94	no	1	yes
	-	-	1	yes
FINGER STRIPS (LHS + RHS)	4-90	no	1 + 2	no
	5-91	no	1	no
	1-92	no	1	no
	3-92	no	1	no
	7-93	no	1	no
	9-93	no	1	no
	3-94	yes/no	1 + 2	no
	5-94	yes/yes	1	no
	8-94	yes/yes	1	yes
	13-94	no	1	no
	14-94	no	1 + 2	no
	15-94	no	1 + 2	no
ANGLES	4-91	no	1	yes
	1-94	yes/no	1	yes
	9-94	no	1	yes

^{*)} 1 = visual inspection
2 = eddy current inspection



Table 2 Proposed P- and b-values for turbulence model [29]

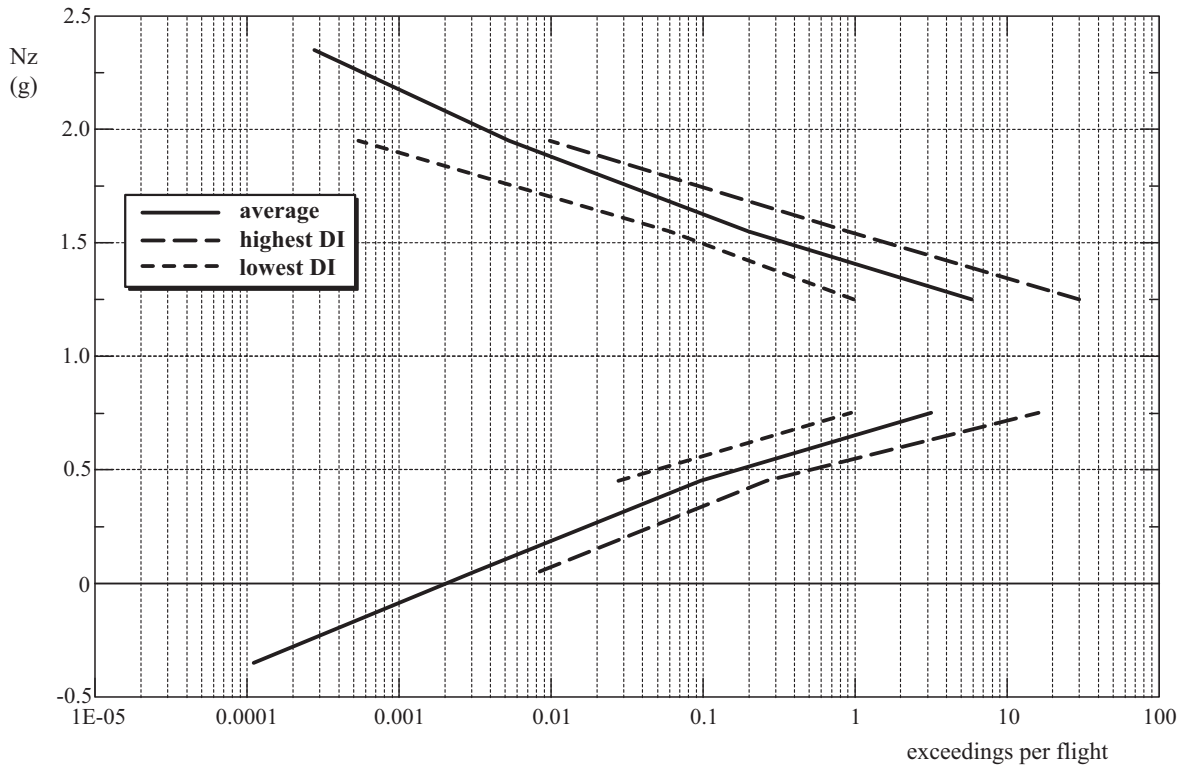
- "Von Karman"-PSD function.
- $L = 2500$ ft for all altitudes.

P-values:

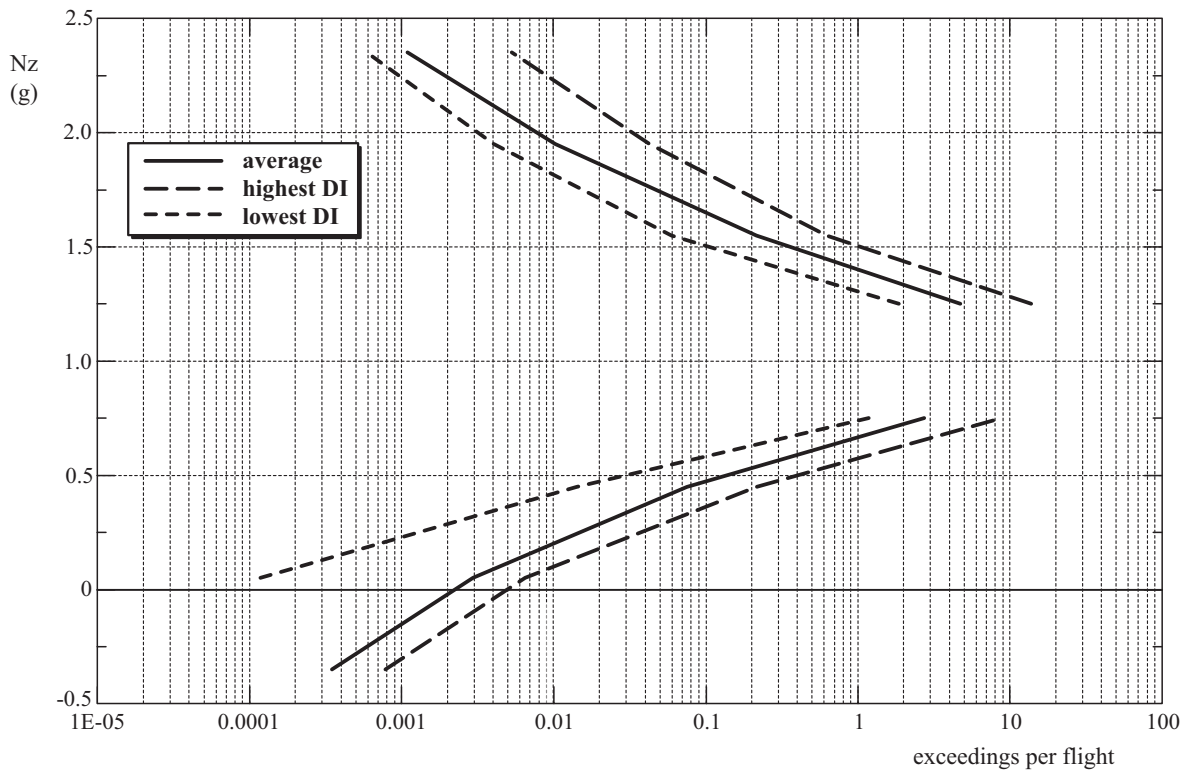
- P_1 : 0.5 at 0 ft, log-linearly decreasing to 9×10^{-3} at 12000 ft.
 9×10^{-3} at 12000 ft, log-linearly decreasing to 1.3×10^{-3} at 30000 ft.
 1.3×10^{-3} above 30000 ft.
- P_2 : 4×10^{-3} at 0 ft, log-linearly decreasing to 2.3×10^{-4} at 12000 ft.
 2.3×10^{-4} at 12000 ft, log-linearly decreasing to 2×10^{-5} at 30000 ft.
 2×10^{-5} above 30000 ft.

b-values:

- b_1 : 1.55 m/s TAS for all altitudes.
- b_2 : 2 m/s TAS at 0 ft, linearly increasing to 2.9 m/s TAS at 20000 ft.
 2.9 m/s TAS above 20000 ft.

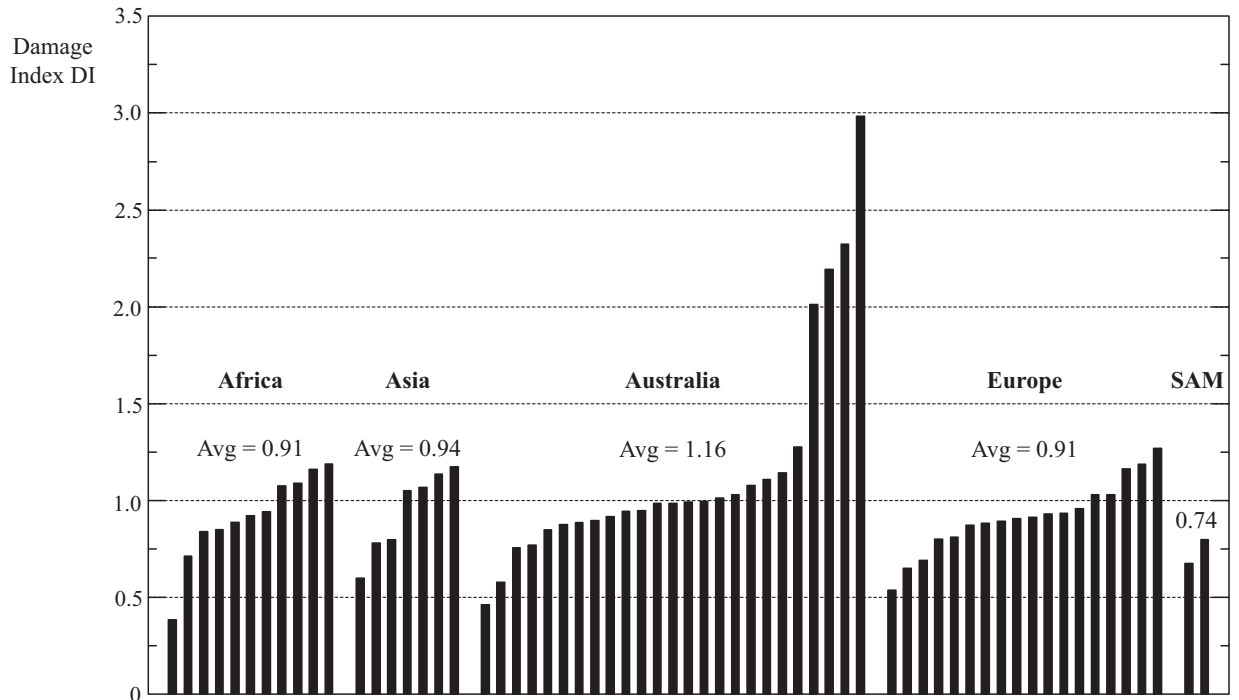


a) F27 Data Base

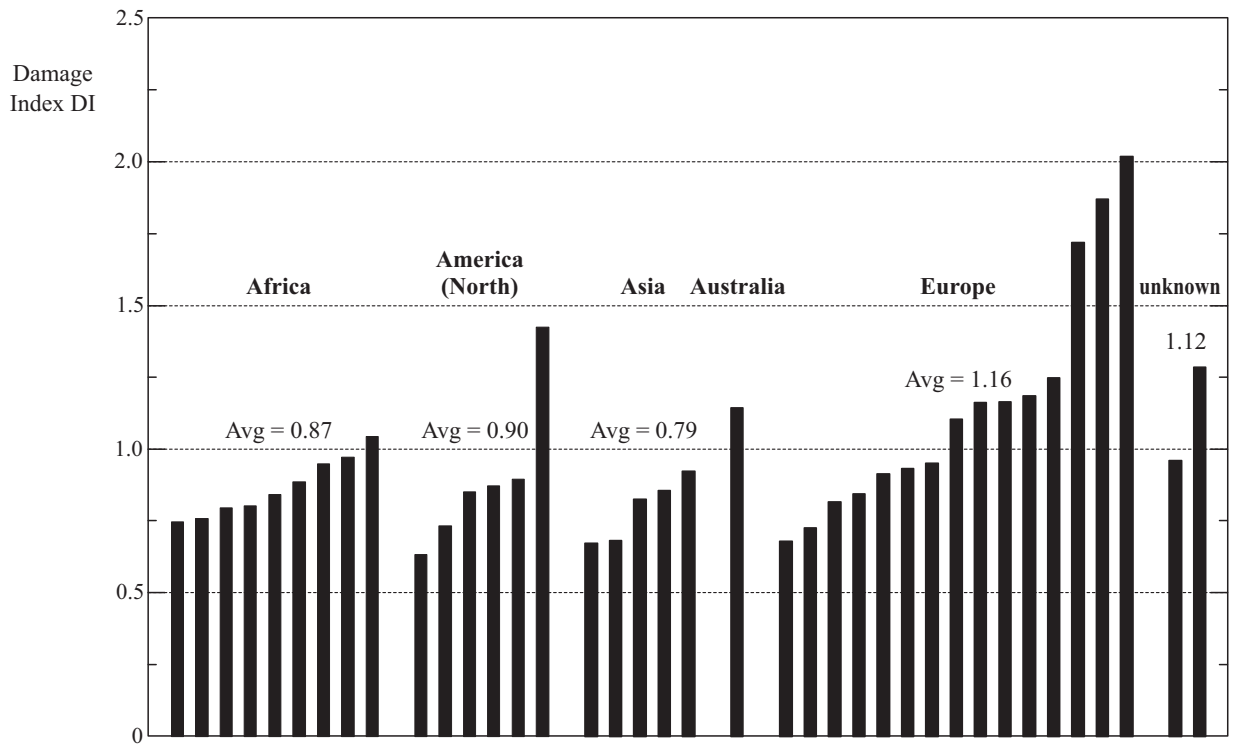


b) F28 Data Base

Figure 1 Variation in load factor experience per aircraft



a) F27 Data Base



b) F28 Data Base

Figure 2 Variation in Damage Index per aircraft

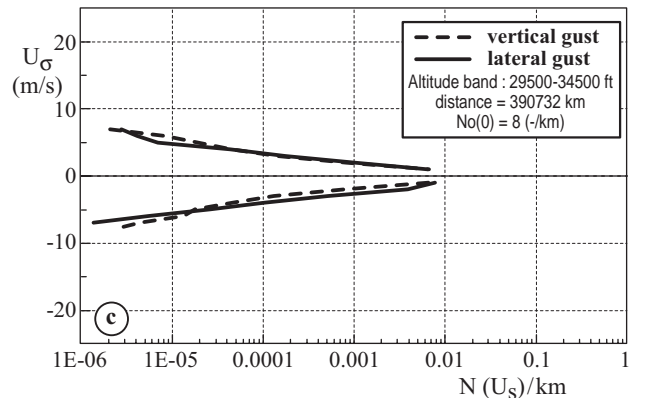
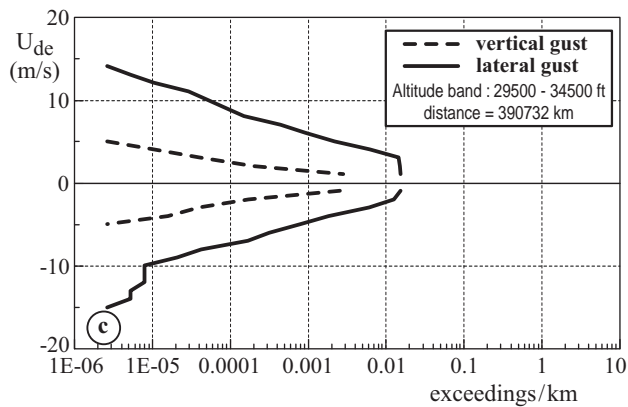
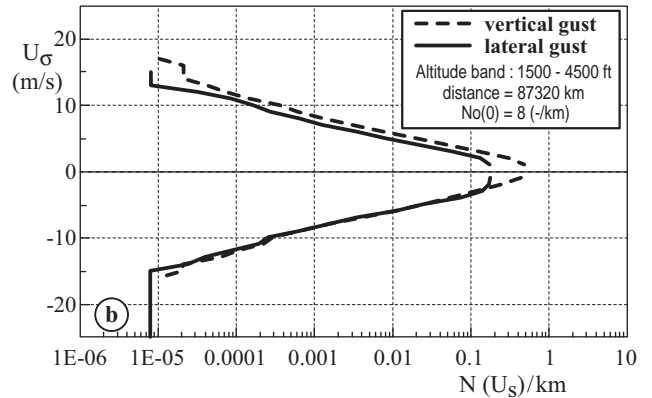
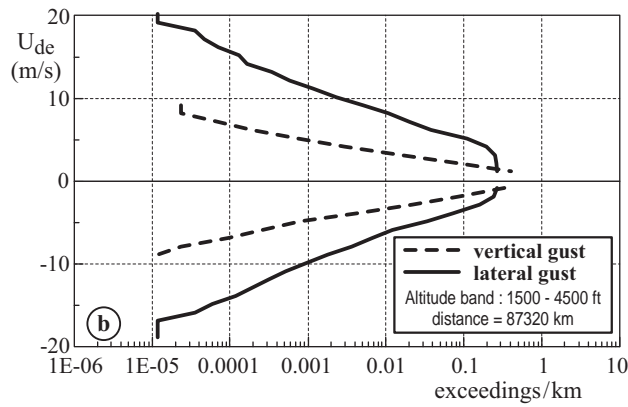
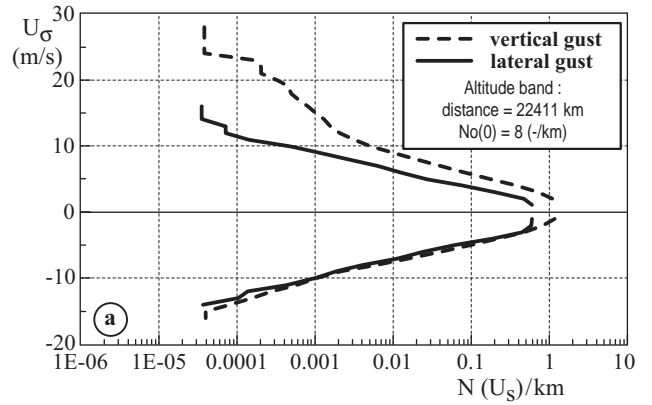
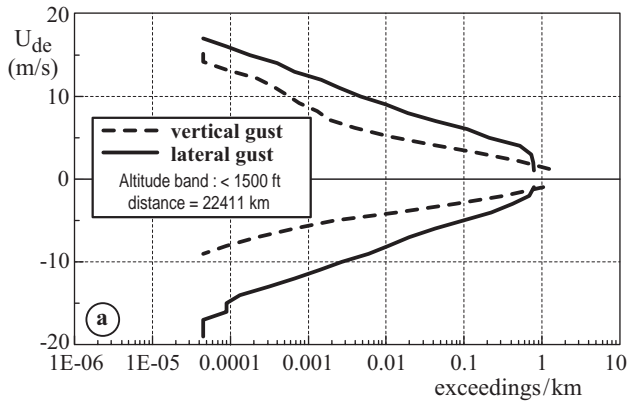


Figure 3 Comparison of lateral & vertical U_{de}

Figure 4 Comparison of vertical & lateral U_{σ} 's

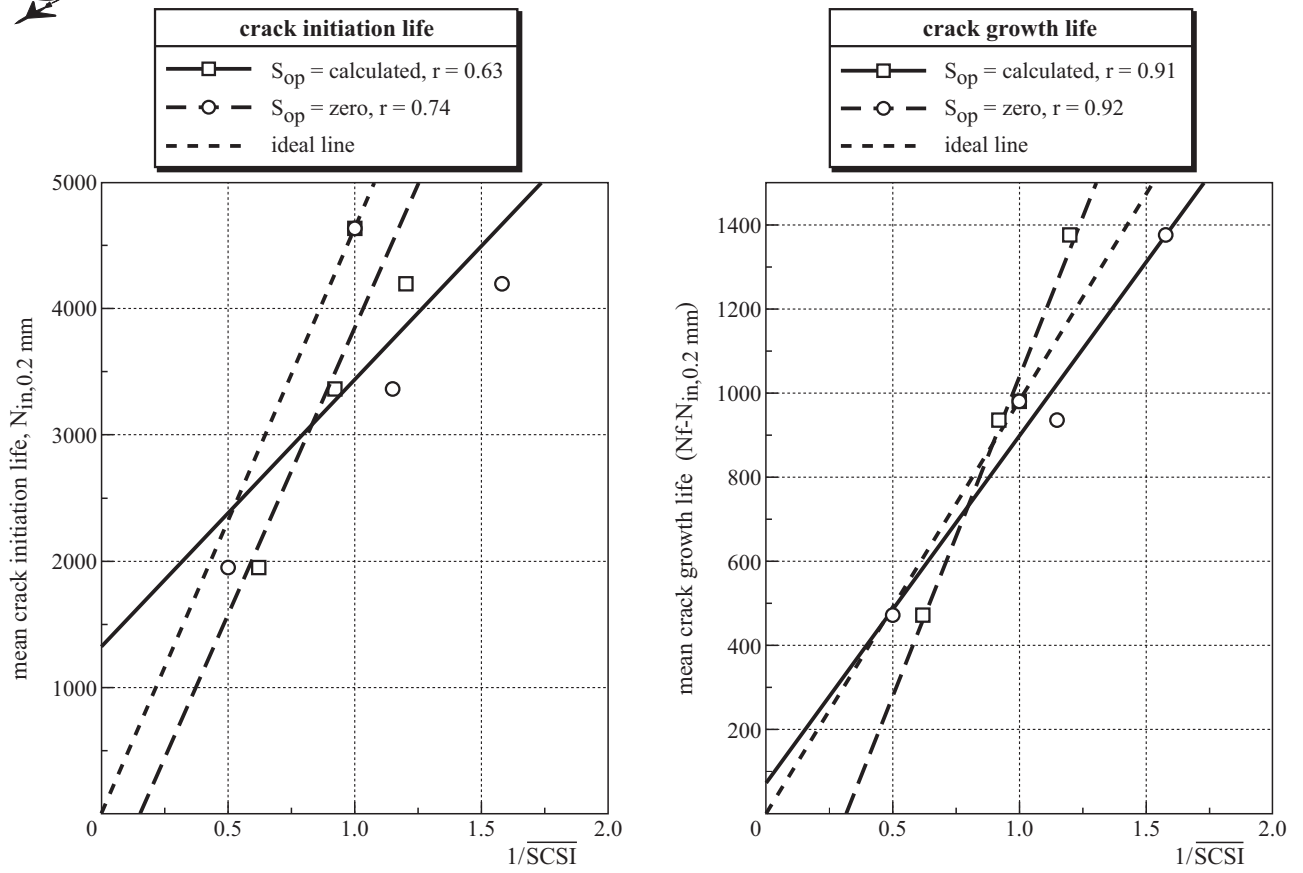


Figure 5 Comparison of effect of minimum opening stress levels on the comparison of calculated SCSI values with crack initiation and crack growth lives

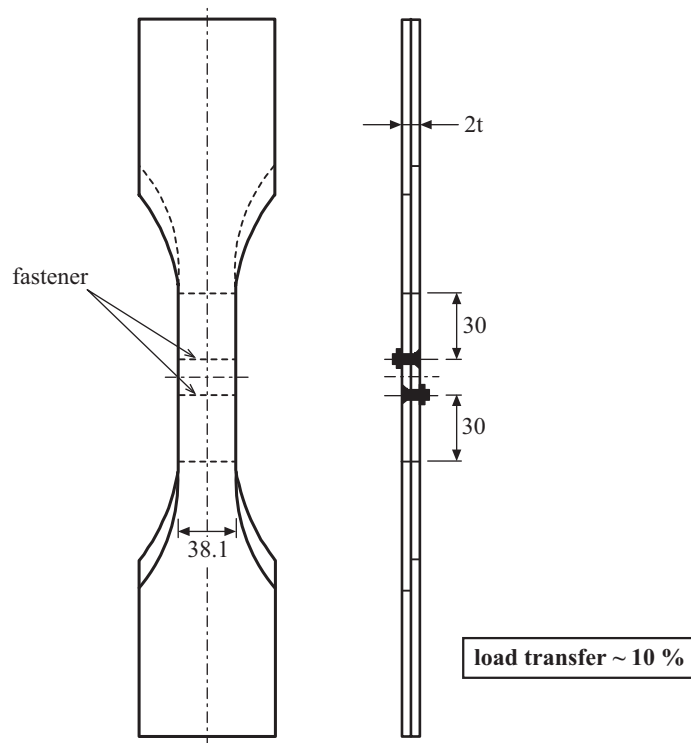


Figure 6 Double dogbone fatigue specimen

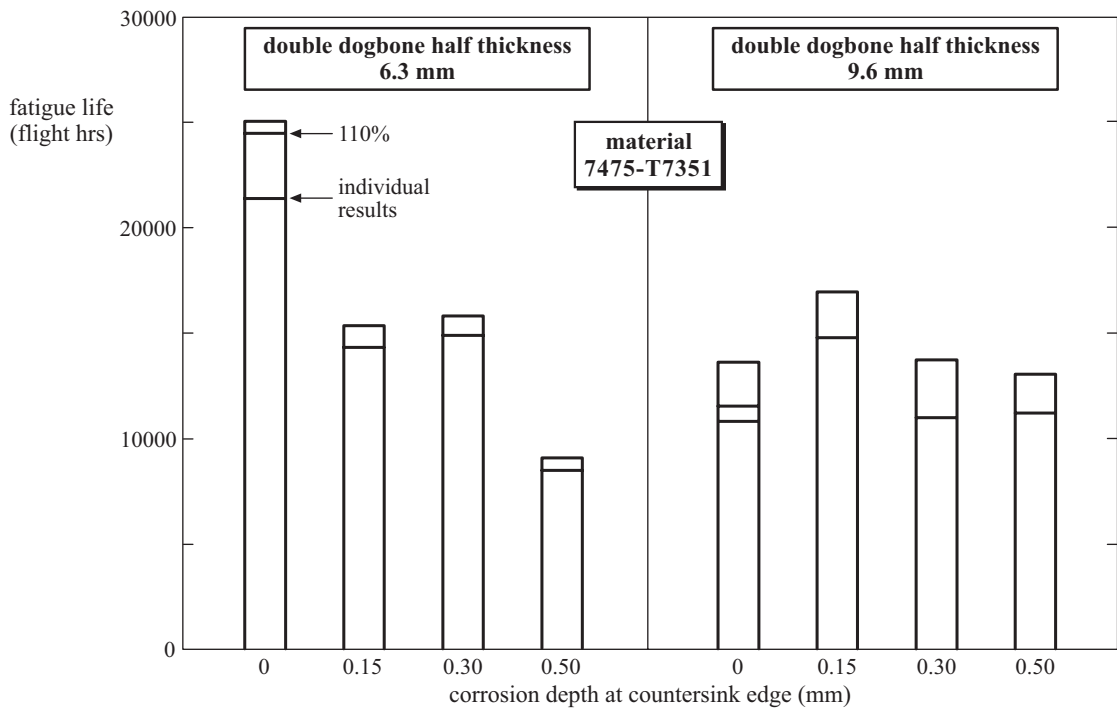


Figure 7 Fatigue lives under manoeuvre loading (120% Basic Leeuwarden) after previous corrosion

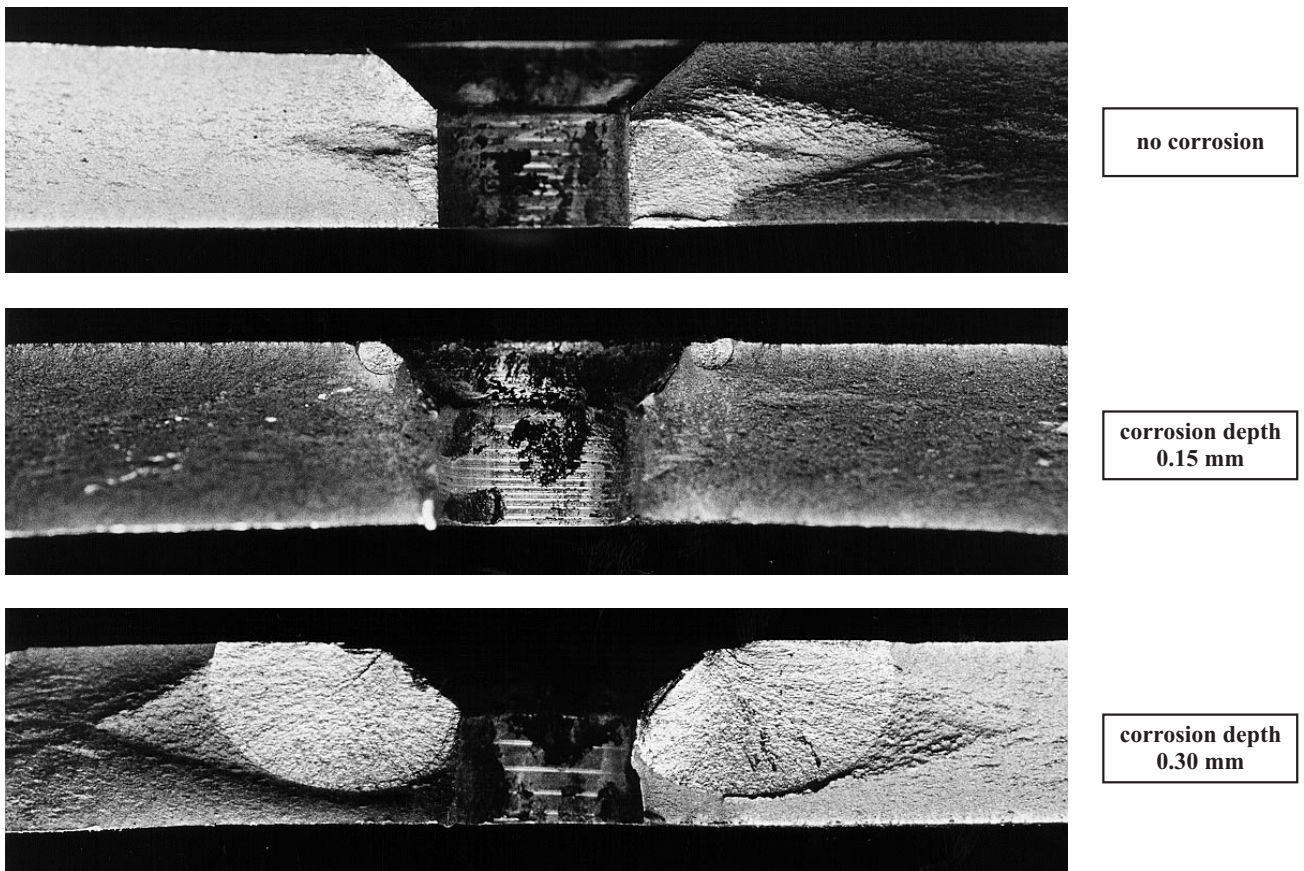
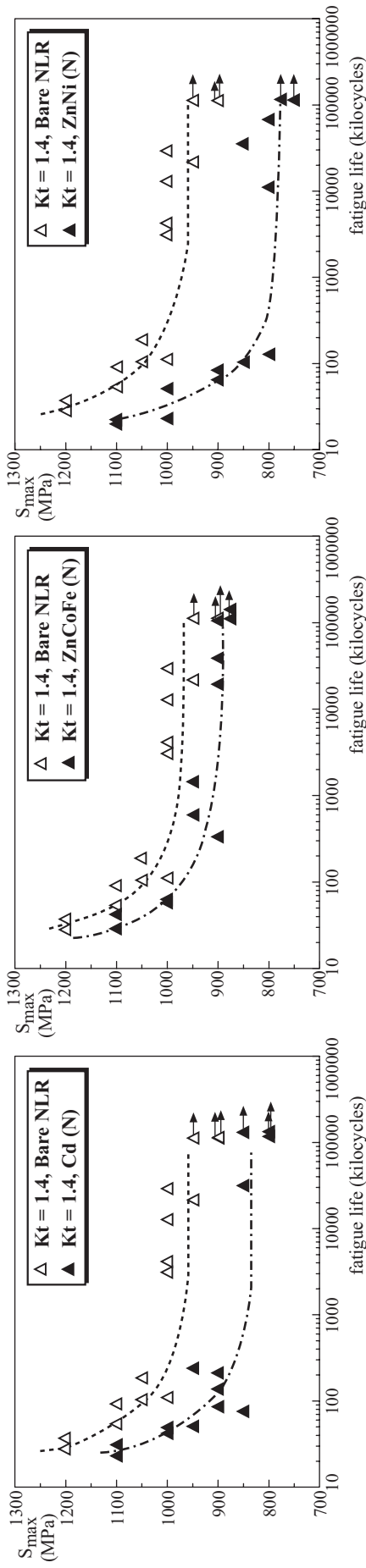


Figure 8 Examples of fatigue crack initiation in uncorroded and corroded joint specimens (half specimen thickness 6.3 mm)



c) Coat 9

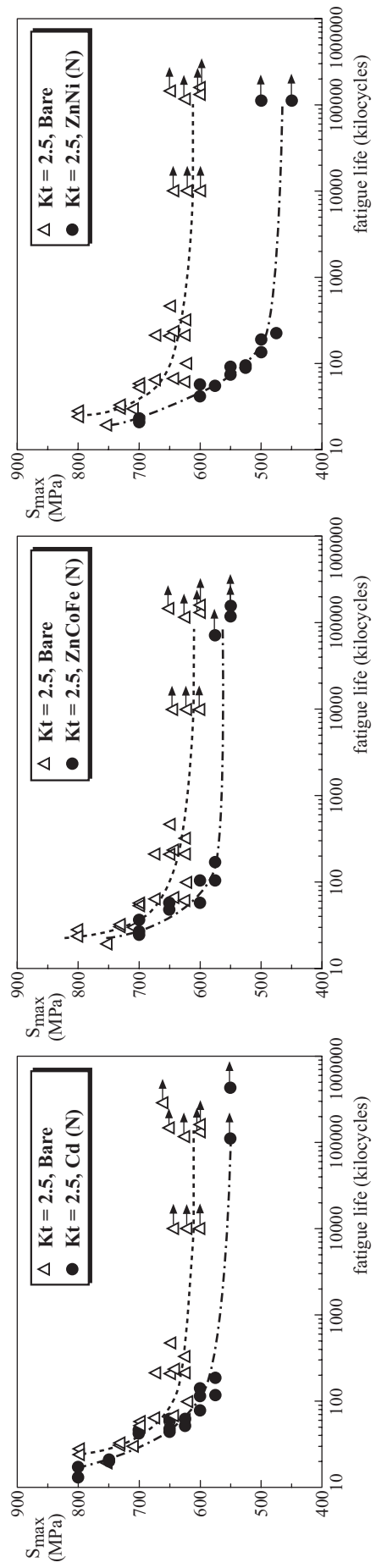


Figure 9 Constant amplitude test results for cadmium, ZnNi and ZnCoFe coated AISI 4340 specimens in comparison with uncoated specimens (bare)

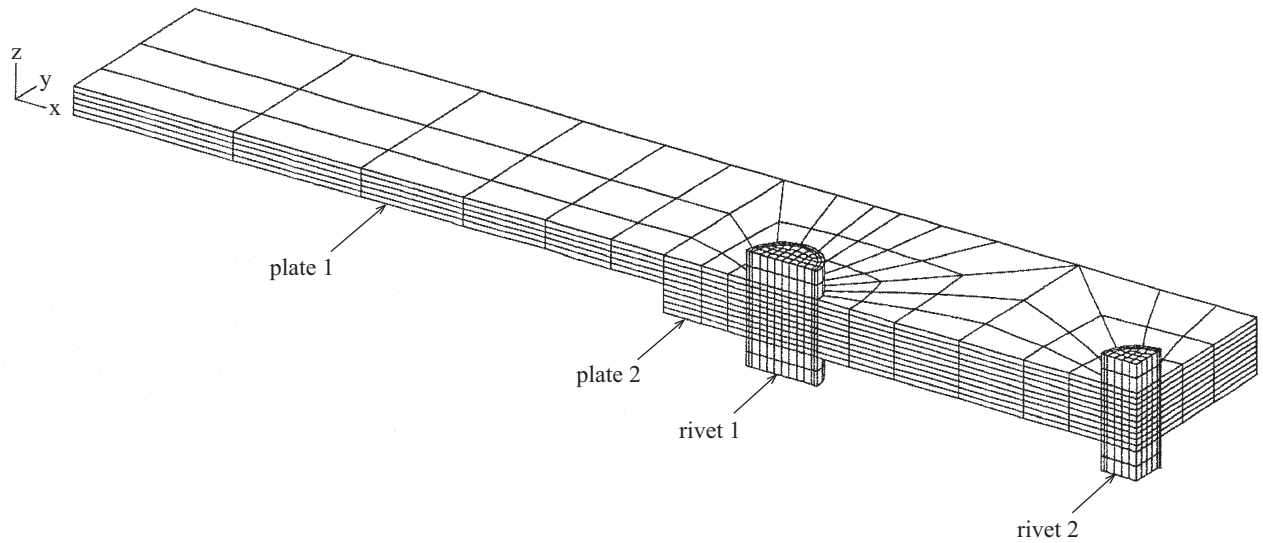


Figure 10 One quarter FE model of a riveted lap joint with three rows of rivets

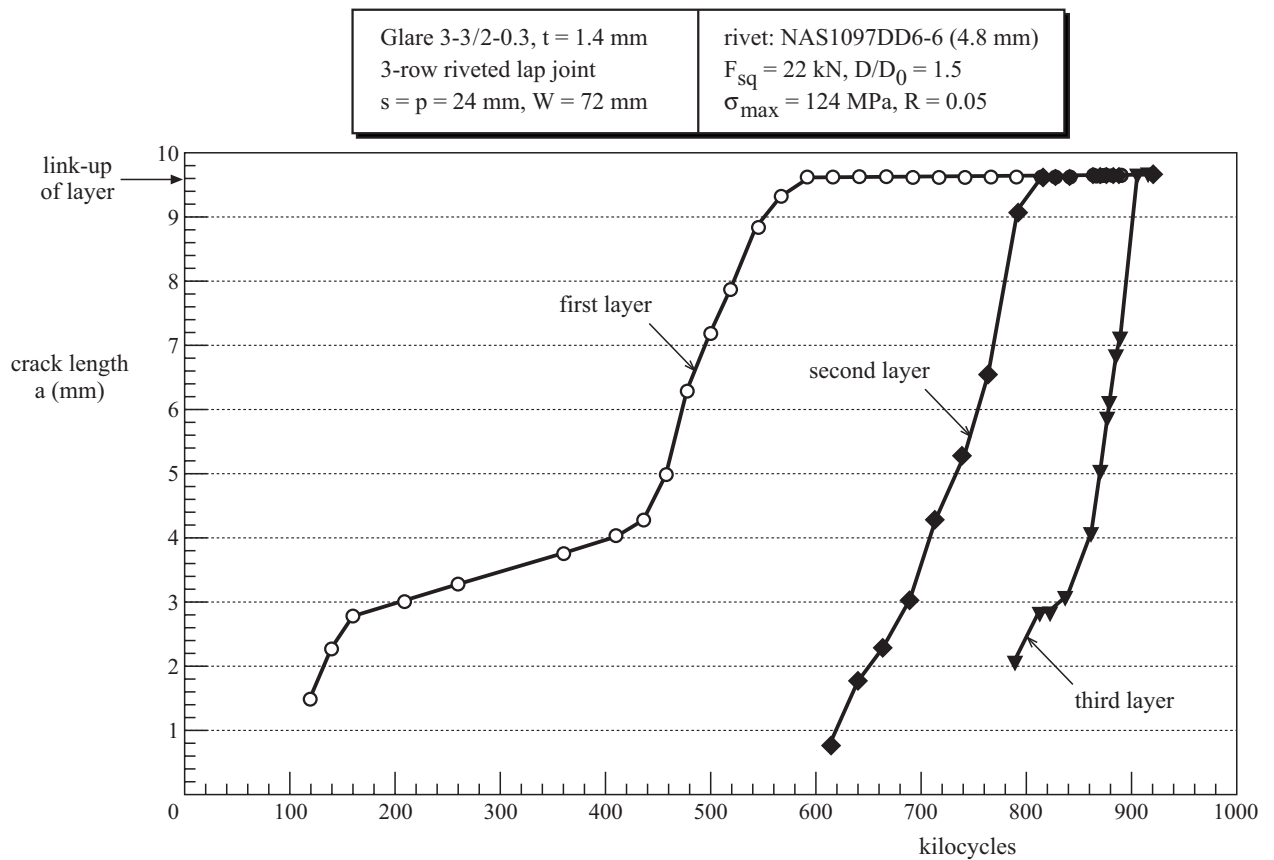


Figure 11 Fatigue crack initiation and crack growth behaviour for a GLARE 3 riveted lap joint for a moderate squeeze force (rivet pitch 24 mm, rivet diameter 4.8 mm) [4]



Fokker 100 horizontal stabilizer-fin test set-up

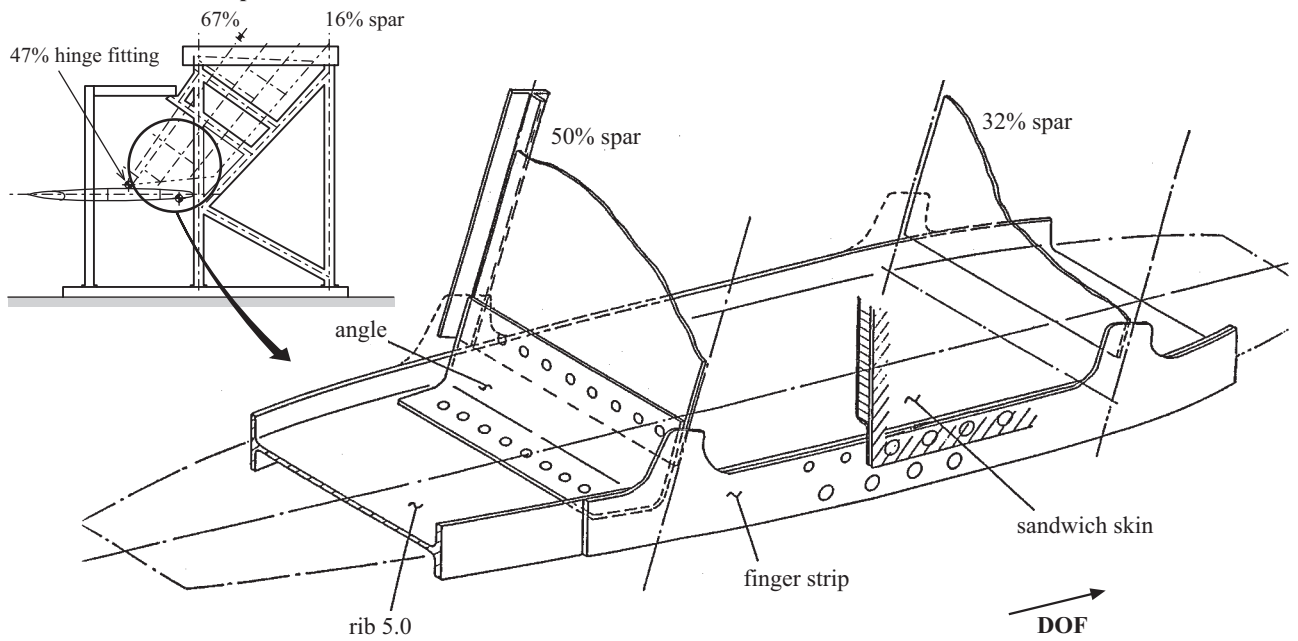


Figure 12 Elements of Fokker 100 fin examined during tear down inspection

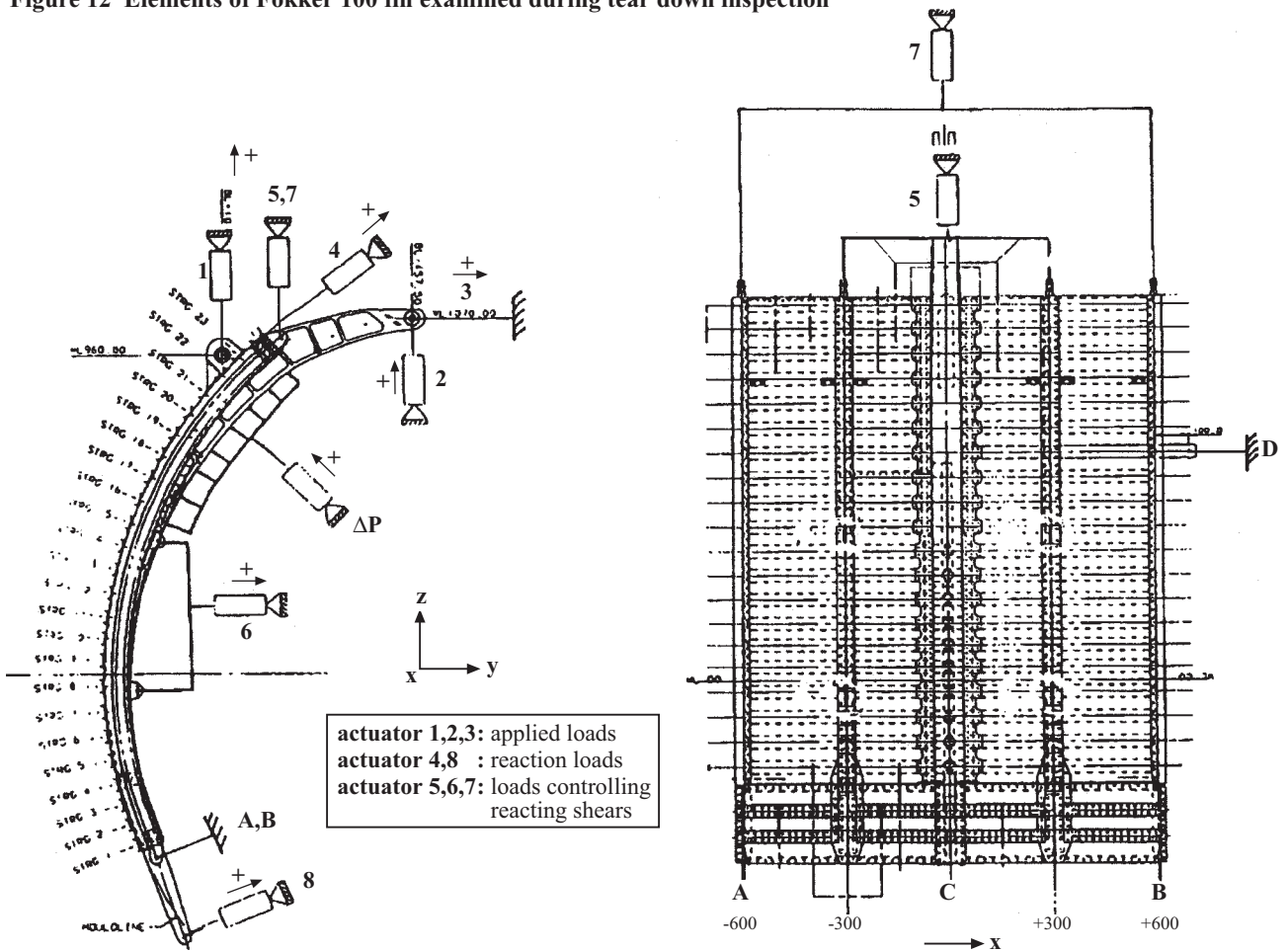


Figure 13 Fokker 60 wingfuselage connection; mainframe componenttest

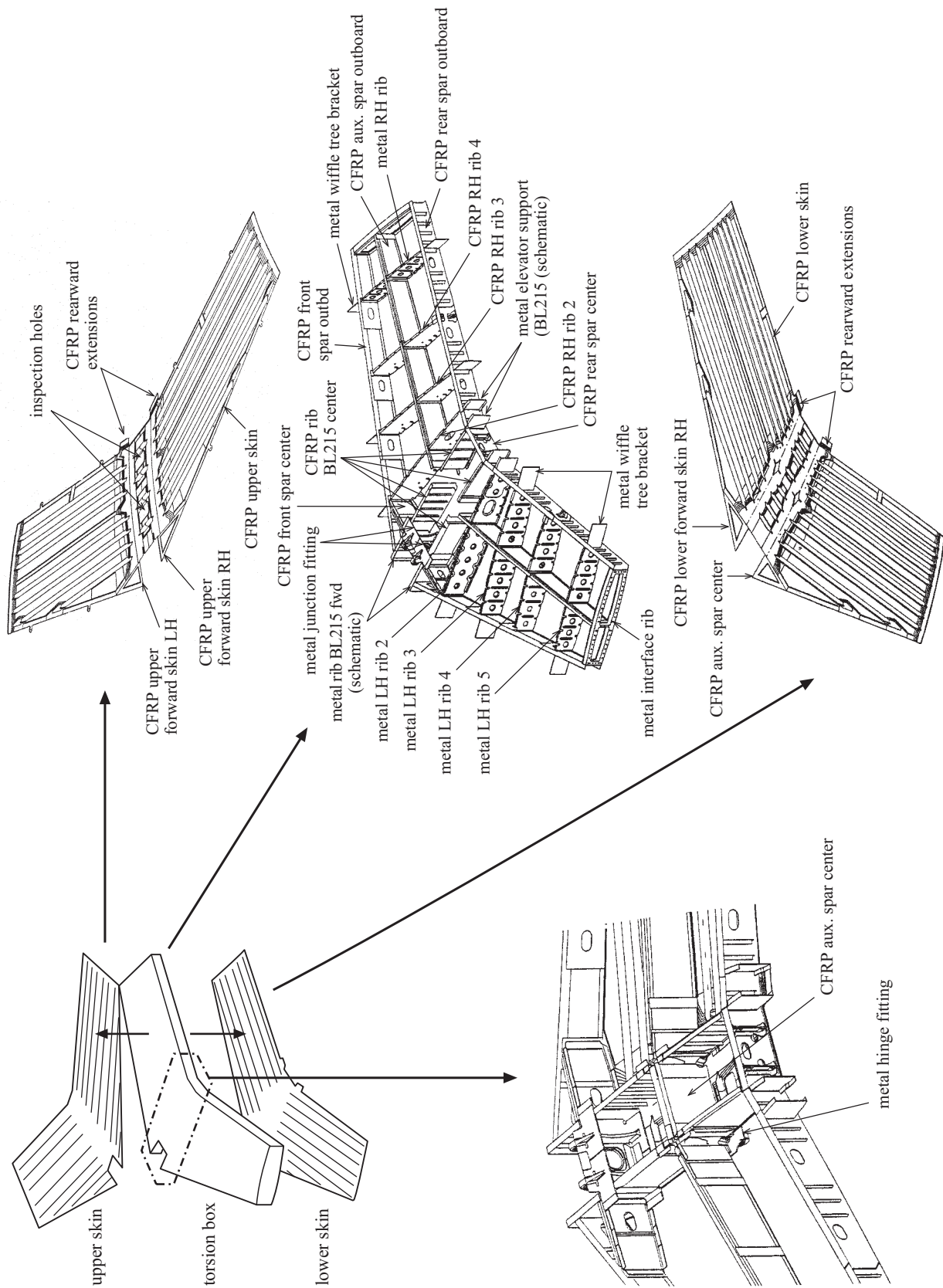


Figure 14 Structural lay-out of the "4-meterbox"

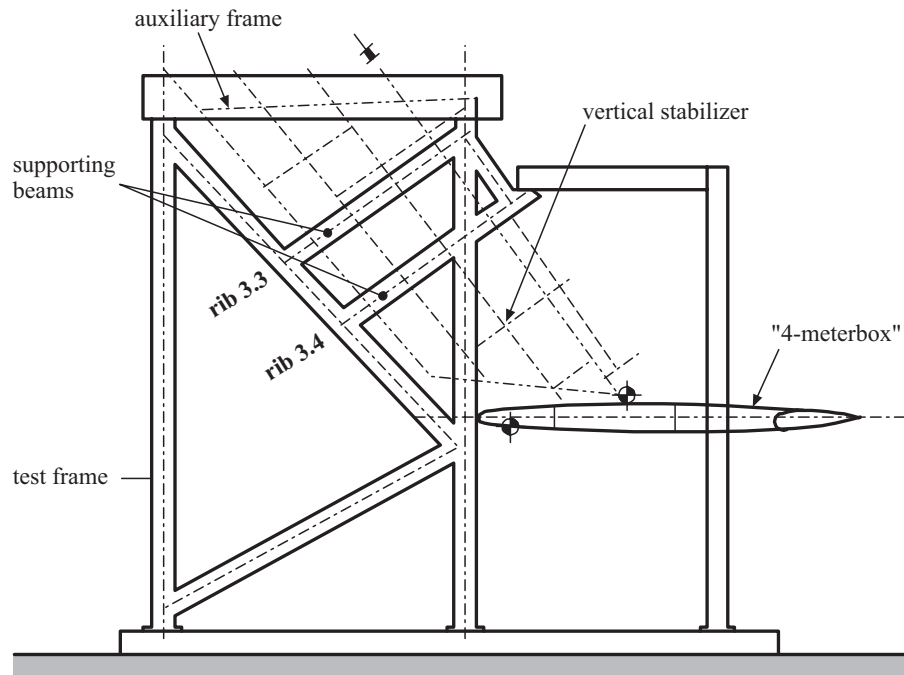


Figure 15 Side view of the test set-up

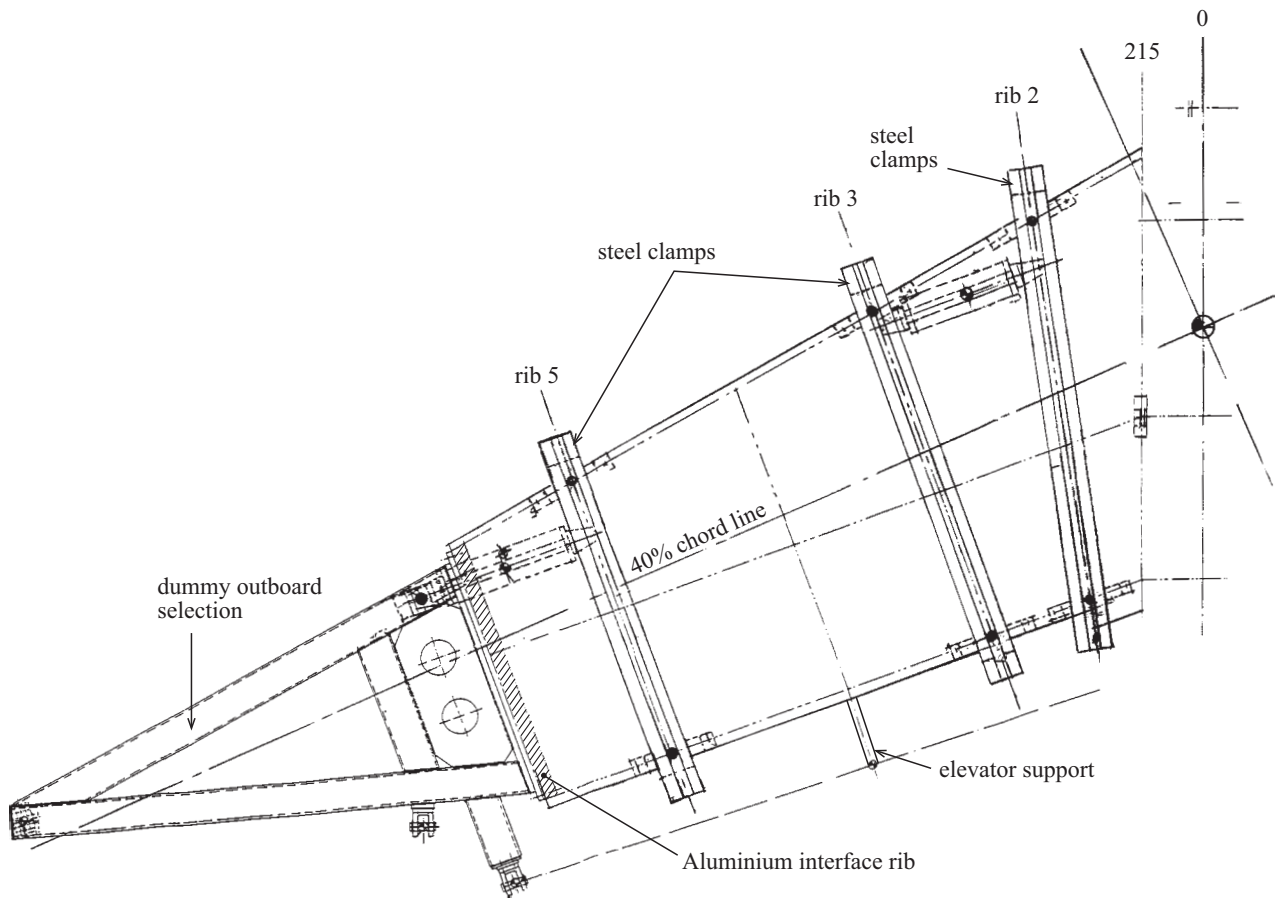


Figure 16 Top view of one side of the "4-meterbox" test set-up

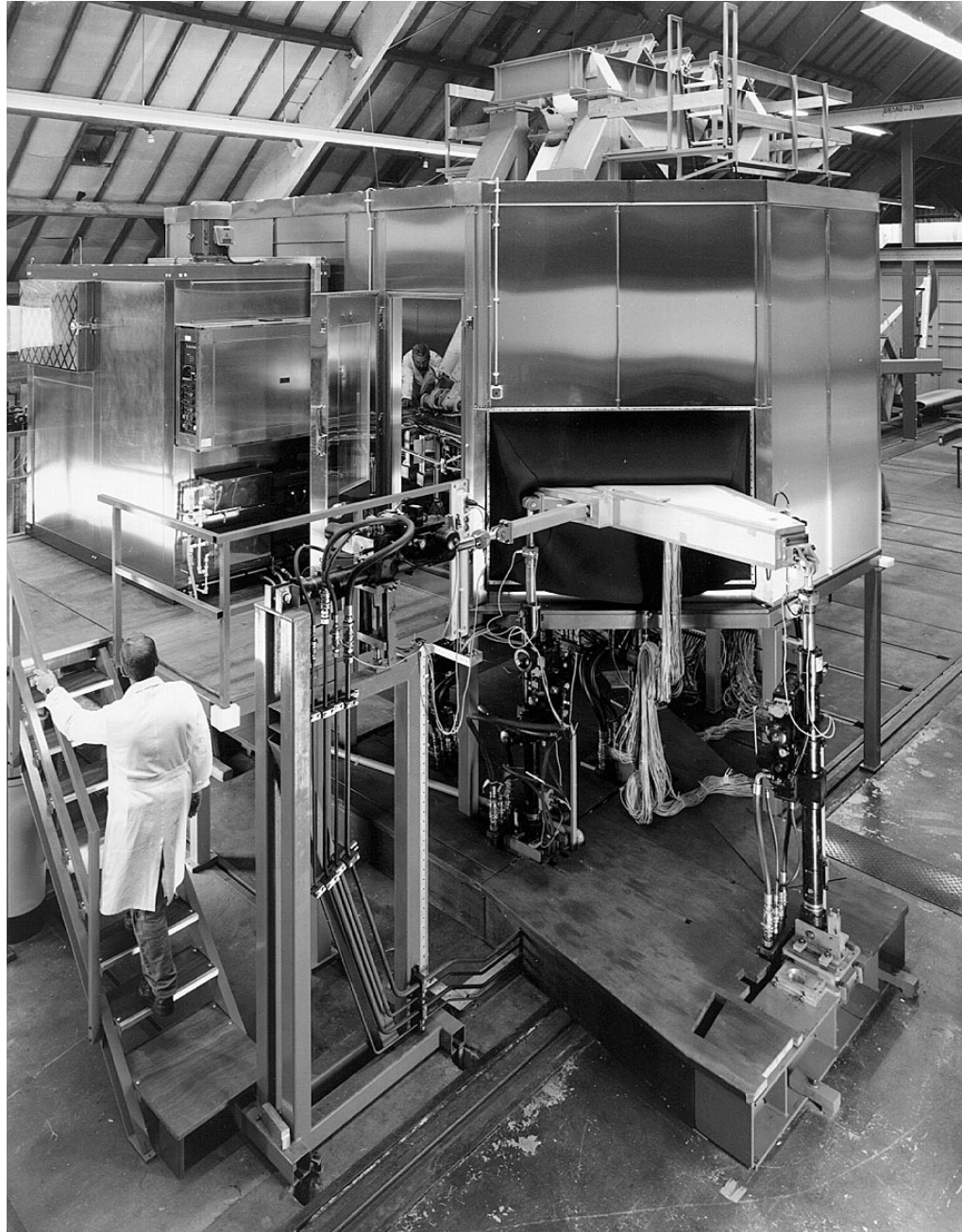


Figure 17 "4-meter box" positioned in the environmental chamber

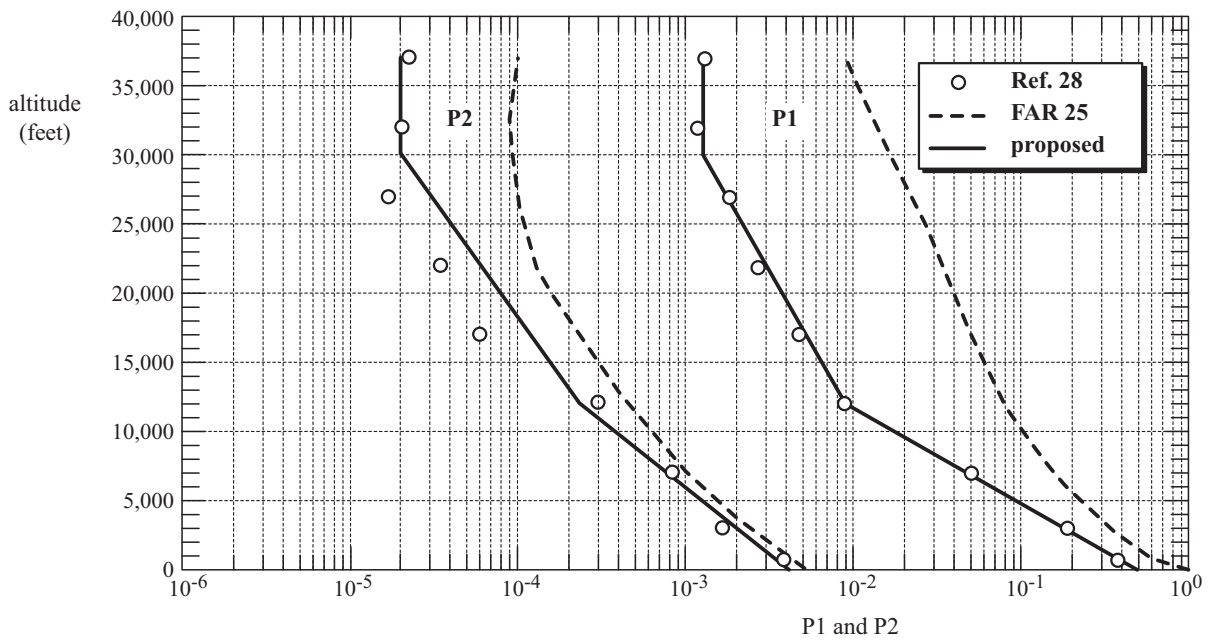
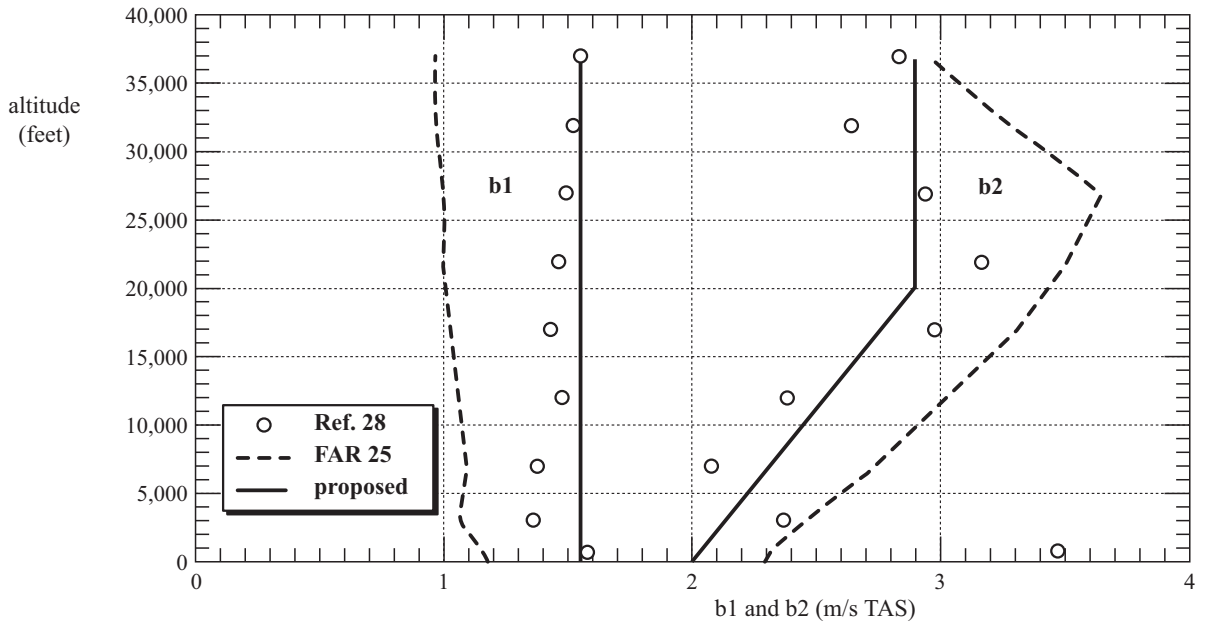


Figure 18 P and b values for proposed gust model [29]

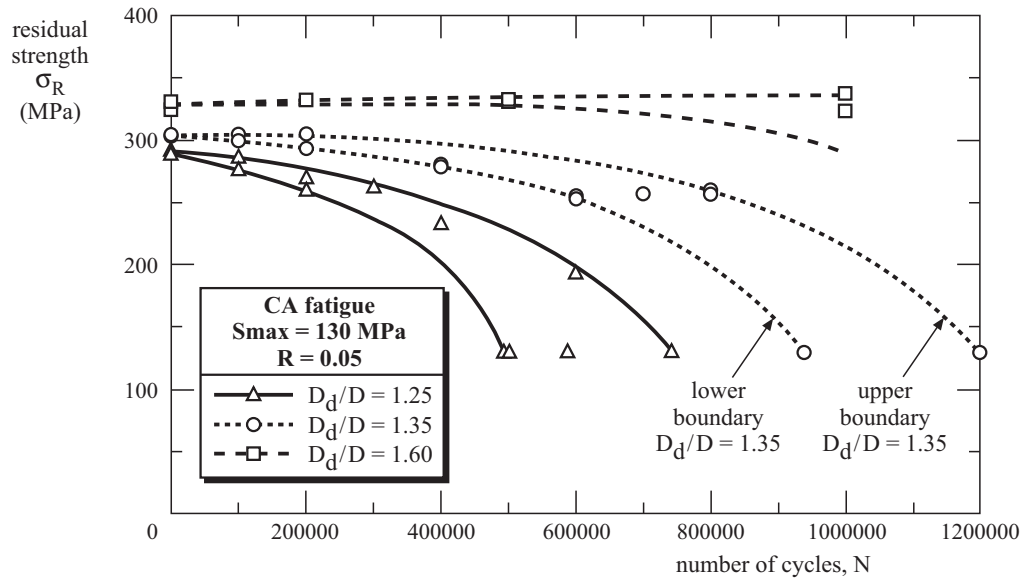


Figure 19 Effect of formed head diameter on the residual strength after constant amplitude fatigue loading. The lines indicate the estimated lower and upper boundaries of the scatterbands

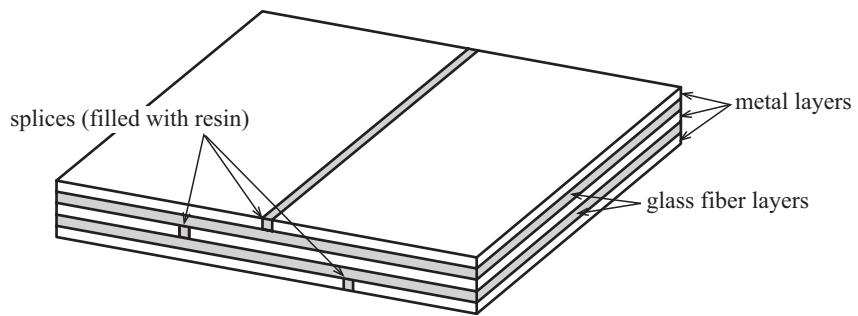


Figure 20 The splicing concept

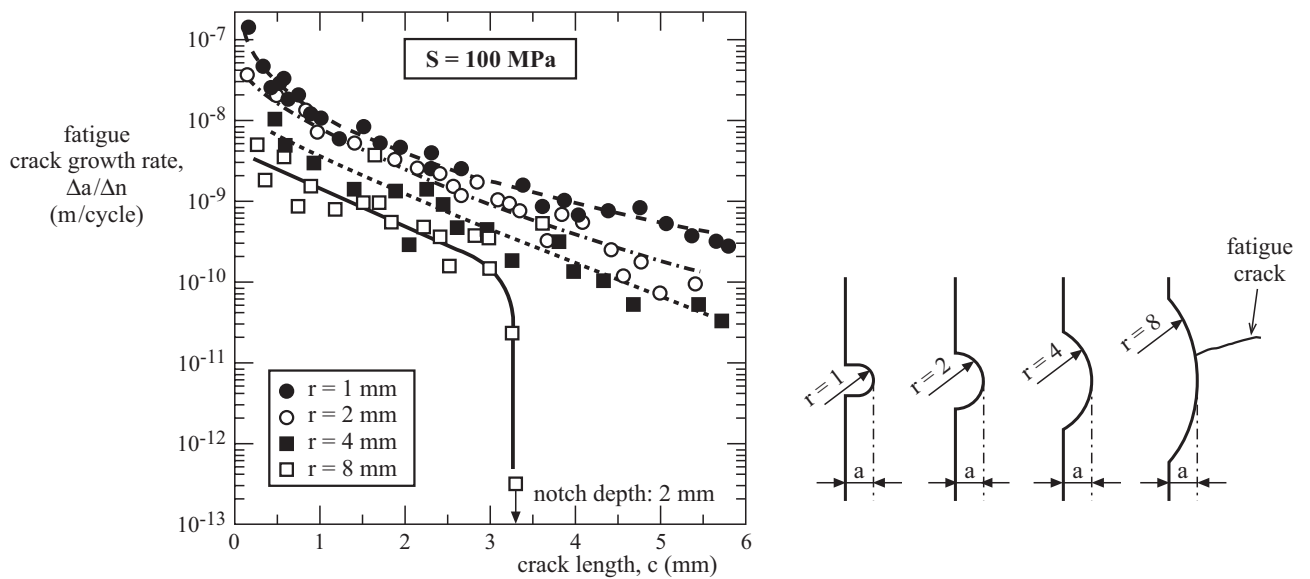


Figure 21 Fatigue crack growth rate in the metal layers versus crack length of cracks emanating from notch root radii of 1, 2, 4 and 8 mm. The specimens were loaded with a nominal stress amplitude of 100 MPa

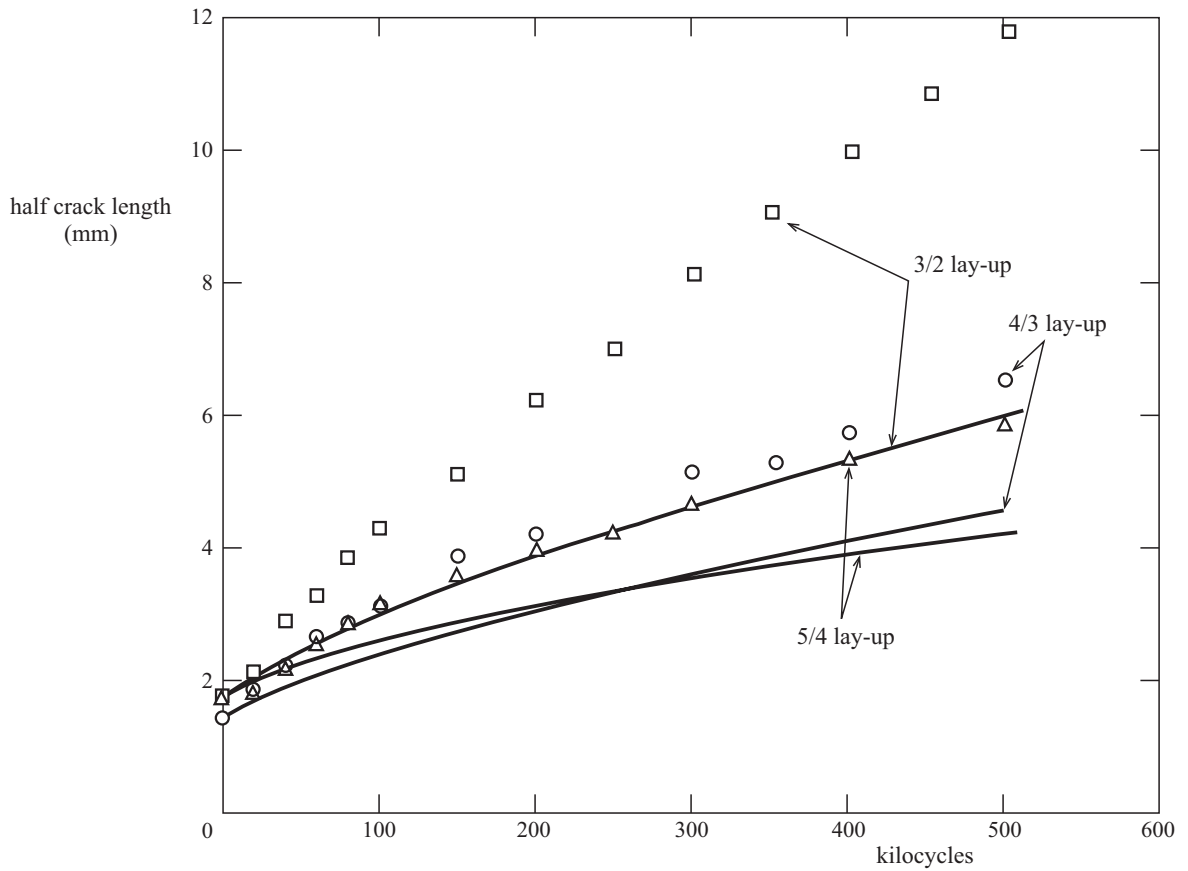


Figure 22a Crack growth curves of GLARE2-0.3 at 120 MPa constant amplitude fatigue loading (R = 0.05, 10 Hz) for several lay-ups

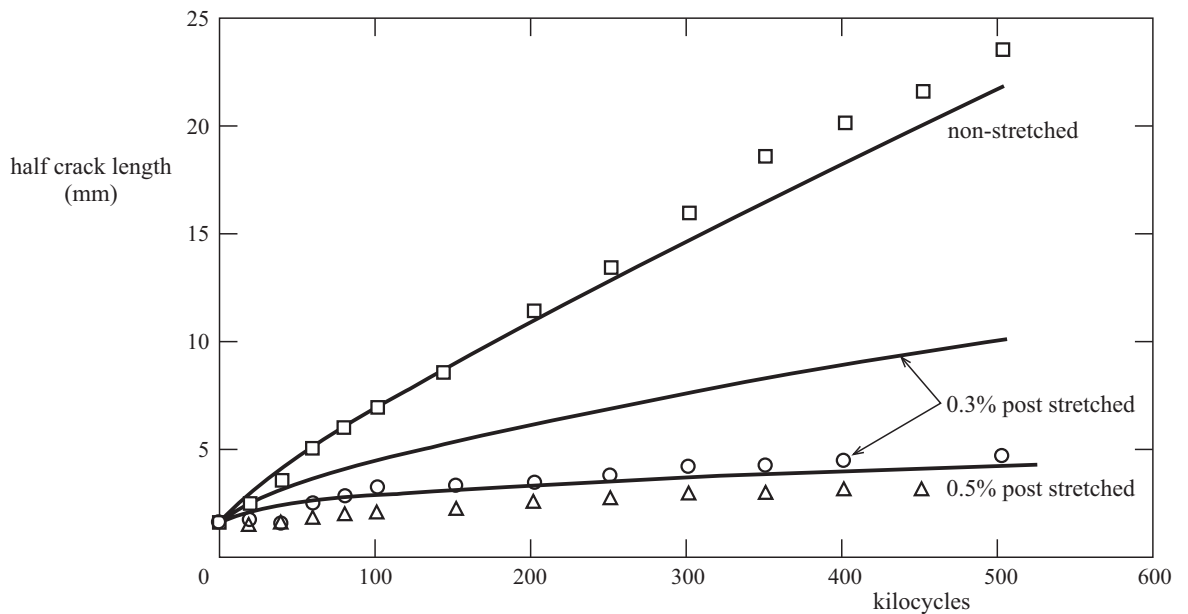


Figure 22b Crack growth curves of GLARE1-3/2-0.3 at 120 MPa constant amplitude fatigue loading (R = 0.05, 10 Hz) for several post stretch percentages